NeuroImage 214 (2020) 116715

Contents lists available at ScienceDirect

NeuroImage

journal homepage: www.elsevier.com/locate/neuroimage

The human connectome project for disordered emotional states: Protocol and rationale for a research domain criteria study of brain connectivity in young adult anxiety and depression

Leonardo Tozzi [a,1], Brooke Staveland [a,1], Bailey Holt-Gosselin [a,1], Megan Chesnut [a], Sarah E. Chang [a], David Choi [a], Melissa Shiner [a], Hua Wu [b], Garikoitz Lerma-Usabiaga [c,d], Olaf Sporns [e], Deanna M. Barch [f], Ian H. Gotlib [c,2], Trevor J. Hastie [g,2], Adam B. Kerr [b,h,2], Russell A. Poldrack [c,2], Brian A. Wandell [b,2], Max Wintermark [i,2], Leanne M. Williams [a,j,*]

[a] Psychiatry and Behavioral Sciences, Stanford University, Stanford, CA, USA
[b] Center for Cognitive and Neurobiological Imaging, Stanford University, CA, USA
[c] Psychology, Stanford University, CA, USA
[d] BCBL. Basque Center on Cognition, Brain and Language, Donostia - San Sebastián, Gipuzkoa, Spain
[e] Psychological and Brain Sciences, Indiana University, IN, USA
[f] Psychological and Brain Sciences, Psychiatry & Radiology Washington University in St. Louis, MO, USA
[g] Statistics, Stanford University, CA, USA
[h] Department of Electrical Engineering, Stanford University, CA, USA
[i] Radiology, Stanford University, CA, USA
[j] Sierra-Pacific Mental Illness Research, Education, and Clinical Center (MIRECC) Veterans Affairs Palo Alto Health Care System, Palo Alto, CA, USA

ARTICLE INFO

Keywords:
Human connectome project
Functional brain imaging
Depression
Anxiety

ABSTRACT

Through the Human Connectome Project (HCP) our understanding of the functional connectome of the healthy brain has been dramatically accelerated. Given the pressing public health need, we must increase our understanding of how connectome dysfunctions give rise to disordered mental states. Mental disorders arising from high levels of negative emotion or from the loss of positive emotional experience affect over 400 million people globally. Such states of disordered emotion cut across multiple diagnostic categories of mood and anxiety disorders and are compounded by accompanying disruptions in cognitive function. Not surprisingly, these forms of psychopathology are the leading cause of disability worldwide. The Research Domain Criteria (RDoC) initiative spearheaded by NIMH offers a framework for characterizing the relations among connectome dysfunctions, anchored in neural circuits and phenotypic profiles of behavior and self-reported symptoms. Here, we report on our Connectomes Related to Human Disease protocol for integrating an RDoC framework with HCP protocols to characterize connectome dysfunctions in disordered emotional states, and present quality control data from a representative sample of participants. We focus on three RDoC domains and constructs most relevant to depression and anxiety: 1) *loss* and *acute threat* within the Negative Valence System (NVS) domain; 2) *reward valuation* and *responsiveness* within the Positive Valence System (PVS) domain; and 3) *working memory* and *cognitive control* within the Cognitive System (CS) domain. For 29 healthy controls, we present preliminary imaging data: functional magnetic resonance imaging collected in the resting state and in tasks matching our constructs of interest ("Emotion", "Gambling" and "Continuous Performance" tasks), as well as diffusion-weighted imaging. All functional scans demonstrated good signal-to-noise ratio. Established neural networks were robustly identified in the resting state condition by independent component analysis. Processing of negative emotional faces significantly activated the bilateral dorsolateral prefrontal and occipital cortices, fusiform gyrus and amygdalae. Reward elicited a response in the bilateral dorsolateral prefrontal, parietal and occipital cortices, and in the striatum. Working memory was associated with activation in the dorsolateral prefrontal, parietal, motor, temporal and insular cortices, in the striatum and cerebellum. Diffusion tractography showed consistent profiles of fractional

* Corresponding author. Department of Psychiatry and Behavioral Sciences, Stanford University School of Medicine, Stanford, CA, 94305, USA.
E-mail address: leawilliams@stanford.edu (L.M. Williams).
[1] These authors contributed equally to this work as first authors.
[2] These authors contributed equally to this work and are listed in alphabetical order by last name.

https://doi.org/10.1016/j.neuroimage.2020.116715
Received 6 February 2020; Accepted 3 March 2020
Available online 5 March 2020

anisotropy along known white matter tracts. We also show that results are comparable to those in a matched sample from the HCP Healthy Young Adult data release. These preliminary data provide the foundation for acquisition of 250 subjects who are experiencing disordered emotional states. When complete, these data will be used to develop a neurobiological model that maps connectome dysfunctions to specific behaviors and symptoms.

1. Introduction

Emotional disorders such as depression, generalized anxiety, social anxiety and phobias affect over 400 million people globally and are the leading cause of disability (Whiteford et al., 2013). In the US alone, the suicide rate among young adults ages 15–24 has tripled since the 1950s (Murphy et al., 2017); moreover, depression exacts an annual cost of $201 billion (Roehrig, 2016). In a recent review, we documented the highly prevalent comorbidity of these emotional disorders, which compounds their impact (Goldstein-Piekarski et al., 2016; Gorman, 1996). Indeed, these disorders share common features such as experiences of increased negative affect (sad mood, negative biases, anxiety), decreased positive affect (anhedonia), and cognitive impairments (poor working memory and cognitive control, ruminations).

There is an urgent public need to reduce the enormous burden of emotional disorders. One fundamental step to do so is the development of biological models for their more effective classification and treatment. Motivated by this goal we launched the Human Connectome Project for Disordered Emotional States (HCP-DES). Based on accumulating evidence from human neuroimaging, our premise is that dysfunctions in networks that govern emotional and cognitive processes contribute to the symptoms and behaviors that characterize disordered emotional states (Van Essen and Barch, 2015; Williams, 2017, 2016). Advances in magnetic resonance imaging (MRI) and in computation spearheaded by large collaborative efforts such as the Human Connectome Project (HCP; Van Essen et al., 2013) provide tools that are ideally suited to elucidate the macroscale organization of the brain. As one of the "Human Connectome Studies Related to Human Disease" projects, HCP-DES will take advantage of the infrastructure developed by the HCP for the acquisition, analysis and sharing of data. We will leverage these tools to systematically quantify macroscale networks of regions ("circuits") that characterize emotional disorders at the individual level.

Emotional disorders are traditionally defined by diagnostic criteria that rely on discrete categories of symptoms. Consistent with the Research Domain Criteria (RDoC) framework (Cuthbert and Insel, 2013; Insel et al., 2010), our goal is to instead characterize emotional disorders based on measures that are grounded in cognitive and affective neuroscience and that span various units of analysis. Moving beyond the current categories of diagnosis, the HCP-DES will detail the associations between circuit function and specific profiles of symptoms and behaviors.

In this paper we present an overview of the aims, methods, quality control and data access policy of the HCP-DES, which uses the RDoC framework to quantify transdiagnostic dysfunctions that characterize disordered emotional states. Our goal is to provide a theoretical and methodological foundation for researchers considering downloading the data once it will be shared and to provide a preliminary overview of how results from our imaging data compare data previously released by the HCP.

2. Rationale: an RDoC framework for disordered emotional states

In this section, we outline our hypotheses concerning how disordered emotional states are characterized by dysfunction of constructs within the RDoC negative valence, positive valence and cognitive systems. These constructs will be the targets of our study and will be measured by three units of analysis: circuits, behavior and self-report.

2.1. Unit of analysis: circuits

See Fig. 1 for a meta-analysis-based summary of the circuits involved in each of our systems of interest.

2.1.1. Negative valence systems

Within the negative valence systems domain, we will focus on the constructs of acute and potential threat and loss, given their prominent role in the symptomatology of emotional disorders (Ahmed et al., 2018; Cuthbert and Insel, 2013; Insel et al., 2010). Acute/potential threat and loss share their localization in affective networks that comprise the amygdala, hippocampus, insula, anterior cingulate cortex (ACC) and lateral prefrontal cortex (lPFC; (Kober et al., 2008; Robinson et al., 2014). Altered activation and connectivity of these regions has been consistently observed across multiple diagnostic categories of disordered emotional states, including depression, generalized anxiety, social phobia, specific phobia, and panic (Fonzo et al., 2015; Jaworska et al., 2015; Killgore

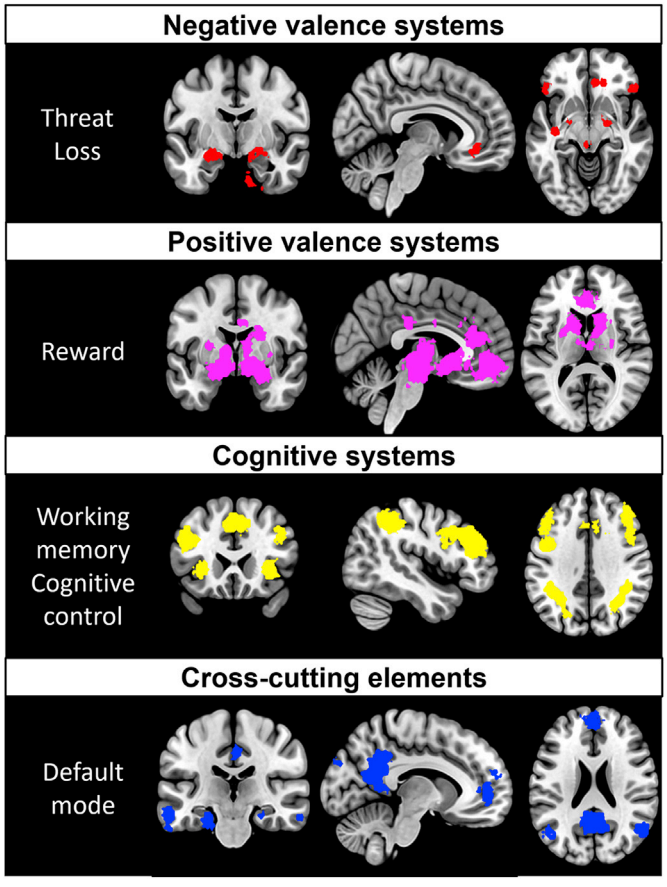

Fig. 1. Meta-analytic activation maps associated with our RDoC constructs of interest. A Neurosynth (Yarkoni et al., 2011) search was conducted on the August 21, 2019 to obtain activation maps for the keywords: negative affect (negative valence systems), reward (positive valence systems), working memory and cognitive control (merged into a single cognitive systems map) and default mode (cross-cutting elements). Association Z maps were thresholded at p false discovery rate <0.01.

et al., 2014; Phillips et al., 2003; Price and Drevets, 2009).

2.1.2. Positive valence systems

Because reductions in the inability to feel pleasure is a prominent feature of some emotional disorders, we will focus on the reward valuation and responsiveness constructs within the RDoC positive valence systems domain. Reward processing networks are comprised by the striatum, orbitofrontal cortex (OFC) and ventromedial prefrontal cortex (vmPFC) and ACC (Haber and Knutson, 2010; Keren et al., 2018). When measuring response to reward, depressed individuals show hypo-activation of the striatum correlating to anhedonia (Hamilton et al., 2012; Treadway and Zald, 2011) as well as changes in the activation of the OFC, medial prefrontal/midfrontal regions, and ACC (Dichter et al., 2012; Zhang et al., 2013).

2.1.3. Cognitive systems

Depression and anxiety are associated with cognitive symptoms such as deficits in concentration, failure to inhibit ruminations and difficulties suppressing negative emotions (Lam et al., 2014). Within the cognitive systems domain, we will focus on the constructs of working memory and cognitive control (Cuthbert and Kozak, 2013). These processes are supported by networks including the dorsolateral prefrontal cortex (DLFPC), dorsal parietal cortex (DPC) and precentral gyrus (Niendam et al., 2012). Research by several groups has shown that people with depression hypo-activate the DLPFC and ACC during working memory tasks and related cognitive control tasks (Elliott et al., 1997a,b; Korgaonkar et al., 2013; Siegle et al., 2007). Patients affected by anxiety disorder also show DLPFC hypo-activation during working memory tasks independently of threat, which supports the transdiagnostic nature of this dysfunction (Balderston et al., 2017; Fales et al., 2008). Hyper-connectivity of the DLPFC with the dorsal parietal cortex (DPC) and with the ACC has also been observed in depressed people during working memory tasks (Vasic et al., 2009) and at rest (Shen et al., 2015). This is posited to reflect an inability to engage in working memory or suppress internal thoughts.

2.1.4. Cross-cutting elements

In the RDoC framework, the Default Mode Network (DMN) is a relevant element in multiple systems. During rest, the DMN tends to be up-regulated, and other networks down-regulated. Up-regulation of the DMN at rest is posited to reflect spontaneously generated self-perception and states of readiness for external focus. In this role, the DMN interacts with networks involved in processing of task-evoked responses such as acute threat, reward and working memory (Cole et al., 2014; Fox et al., 2005; Spreng et al., 2013). The DMN is defined by posterior hubs in the posterior cingulate cortex (PCC) and angular gyrus (AG) and an anterior hub centered in anterior medial prefrontal cortex (amPFC) (Greicius et al., 2003; Raichle, 2015). Several studies report functional hyper-activation and hyper-connectivity of the DMN in depression (Hamilton et al., 2015) and anxiety (Qiu et al., 2011). Hyper-activation of the frontal subnetwork of the DMN in particular has been associated with maladaptive rumination (J. P. Hamilton et al., 2011b). DMN interactions with other networks may also exacerbate states of emotional disorder. For example, depression has been associated with positive correlations (rather than anti-correlation) between the DMN and DLFPC working memory networks (Bartova et al., 2015; Hwang et al., 2015; Sheline et al., 2010). This positive correlation may reflect difficulties to suppress ruminative thoughts and focus on tasks.

2.2. Unit of analysis: behavior

2.2.1. Negative valence systems

Behaviorally, acute and potential threat are related to the accuracy of identification of emotional facial expressions. Several studies have shown that individuals suffering from depression are less accurate at identifying all emotions, especially happiness, sadness and neutral (Dalili et al., 2015; Milders et al., 2010; Sanchez et al., 2017; Watters and Williams, 2011). In addition, individuals with anxious depression, compared to those with non-anxious depression, have been shown to have a diminished ability to recognize happy and sad facial expressions (Berg et al., 2016). The RDoC construct of loss is associated with psychomotor retardation and deficits in executive function (Insel et al., 2010). Converging evidence points toward a deficit of executive function in mood disorders as detected by several measures of processing speed, shifting of attention and working memory (Walters and Hines-Martin, 2018).

2.2.2. Positive valence systems

At the behavioral level, positive valence systems are involved in responses to reward. Increasing evidence has characterized depression by reduced positive emotional reactivity (Bylsma et al., 2008) and reward-processing deficits (Eshel and Roiser, 2010). In behavioral studies of reward, individuals with depression showed reduced reward responsiveness (Pechtel et al., 2013) and deficits in reward-based decision making (Kunisato et al., 2012). Reduced reward learning has been also demonstrated in patients with depression reporting high anhedonia compared to those reporting low anhedonia. This deficit has been shown to be associated with worse treatment outcomes (Vrieze et al., 2013).

2.2.3. Cognitive systems

Behavioral correlates of cognitive control impairment include distractibility, impulsive behavior and slower processing of information. Individuals with MDD show cognitive symptoms such as deficits in concentration, failure to inhibit ruminations or inability to suppress negative emotions (Lam et al., 2014). Several studies have linked depression with deficits in psychomotor speed, attention, visual learning and memory, attentional switching, verbal fluency and cognitive flexibility (Lee et al., 2012). Depression has also been associated with impaired cognitive performance on a range of tasks designed to assess executive function, memory and attention (Rock et al., 2014). Similarly, anxious patients also show reduced accuracy and longer reaction times during cognitive tasks (Balderston et al., 2017).

2.3. Unit of analysis: self-report

Questionnaires designed to quantify the severity of anxiety disorders and depression typically contain several items or subscales pertaining to threat, loss, reward, and cognitive function. Pooling items from different questionnaires has been shown to be a reliable method to identify underlying symptom profiles which cut across categorical diagnoses (Grisanzio et al., 2018).

2.3.1. Negative valence systems

Depressed patients usually present with complaints of persistently decreased mood over the course of weeks or even months. They also often note that they tend to interpret neutral or even positive events as negative (negative emotional bias) (Hasler et al., 2004). Other frequently reported symptoms include persistent irritability, pessimism, sadness, hopelessness, self-blame, and guilt (Diagnostic and statistical manual of mental disorders, 2013; Fried and Nesse, 2015).

2.3.2. Positive valence systems

Anhedonia, or loss of pleasure, is a core feature of depression. Self-reported symptoms of anhedonia include reward insensitivity, lack of positive mood and motivation, and loss of interest in positive experiences (Diagnostic and statistical manual of mental disorders, 2013).

2.3.3. Cognitive systems

Cognitive dysfunction encompasses a broad spectrum of common symptoms of depression and anxiety that negatively affect quality of life and impact general functioning. For example, depressed patients often complain about decreased productivity in the workplace, difficulties concentrating, loss of memory and attention deficits (Knight and Baune,

2018). Several studies have shown that subjective reports of cognitive impairment also correlate with symptoms pertaining to other domains, such as decreased mood (Hill et al., 2016).

3. Research aims

The objective of HCP-DES is to use protocols harmonized with the overarching HCP to elucidate the relationship between circuits, behavior and self-reported symptoms cutting across conventional diagnoses of depression and anxiety disorders. We will elucidate these relations using both region-of-interest approaches and data-driven machine-learning.

Drawing on existing knowledge about circuit dysfunction in emotional disorders and the RDoC framework, we hypothesize that disordered emotional states will be associated with the following disruptions detectable at the circuit, behavioral and self-report units of analysis, independent of clinical diagnosis: (a) hypo-connectivity of networks for acute threat, behavioral threat dysregulation and self-reported anxiety symptoms; (b) hypoactivation and hypo-connectivity of networks for reward evaluation/responsiveness, behavioral hypo-responsiveness to social reward and self-reported anhedonia; (c) hypo-activation of networks for working memory, poorer executive function performance and self-reported ruminations (d) dysfunction in brain circuits cross-cutting across all domains. Our secondary sub-aims are to examine whether (i) disruption of functional circuits is related to structural changes in white matter fiber tracts; and (ii) network-symptom-behavior relations predict clinical outcomes relevant to disability and burden of illness over a 1-year follow-up.

4. Protocol: methods and design

4.1. Ethical approval

The Institutional Review Boards of Stanford University has approved this protocol (protocol #41837). A study coordinator thoroughly explains the protocol to participants and answers any questions before they can provide informed consent to begin the study. The study is conducted according to the principles of the Declaration of Helsinki (2008).

4.2. Recruitment and screening

We will recruit 250 individuals experiencing symptoms of emotional distress (clinical participants) and 50 individuals not experiencing any symptoms of emotional distress (healthy controls). Having a large number of clinical participants will allow us to capture the full spectrum of dysfunctions in our constructs of interest and analyze our data as a continuum ranging from the absence of symptoms (represented by our control group) to severe manifestations. Our sample of controls will also help us establish the extent of overlap between measures collected by HCP-DES and HCP-HYA, to potentially use the latter dataset as an extended pool of controls. All participants will be 18–35 years of age in order to obtain data from individuals in the peak age range for emotional disorders and to facilitate harmonization with the HCP Healthy Young Adult dataset (Van Essen et al., 2013).

Participants will be recruited from the surrounding community using flyers and social media advertisements (i.e., Facebook and Instagram Ads). Fig. 2 details the study flow for healthy controls and clinical participants. All participants will respond to an online screening survey reviewed by a study coordinator to determine eligibility. Respondents will provide information concerning demographics, any current or past pharmacotherapy or psychotherapy, their medical history, MRI scanner contraindications, anxiety and depression symptoms, and alcohol or substance use. A summary of all inclusion and exclusion criteria is presented in Table 1. Importantly, levels of clinical symptoms will be assessed by an in-house survey containing items from the DASS, MASQ, BAI, BIS, and RRS scales (see Methods below). The survey is composed of five categories (containing four items in each) selected to match each of

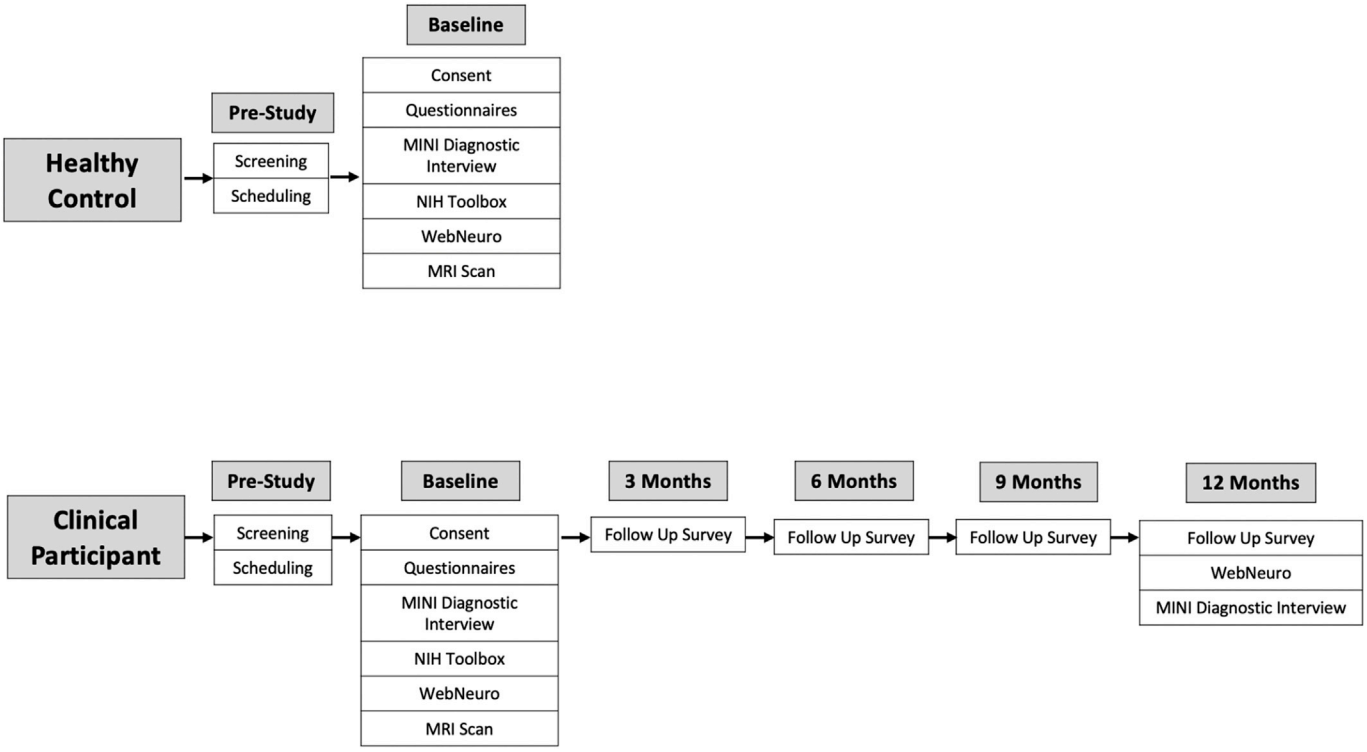

Fig. 2. Study flow for healthy controls and clinical participants. Eligible healthy controls and clinical participants initially fill out an online screening survey, then are scheduled for a visit, and finally conduct the in-person baseline visit. Additionally, clinical participants fill out a brief survey every three months and conduct additional cognitive testing and a clinical interview a year following their in-person baseline visit.

Table 1
Inclusion/Exclusion criteria for clinical participants and healthy control study entry. All participants are screened via an online screening survey that is reviewed by a study coordinator prior to establishing eligibility.

Clinical Participants and Healthy Controls	Clinical Participants Only	Healthy Controls Only
Inclusion Criteria		
● Ages 18-35 ● Fluent and literate in English, and show non-impaired intellectual abilities to ensure adequate comprehension of the task instructions ● Written, informed consent ● fMRI scanning eligibility, including no evidence of any form of metal embedded in the body (e.g., metal wires, nuts, bolts, screws, plates, sutures)	● Report at least a moderate degree of one or more of the following sections: anhedonia, anxious arousal, concentration problems, rumination, tension, as assessed using questions from the MASQ, BAI, RRS, and BIS	● No significant history of any psychiatric disorders, substance abuse, neurological disorders, or cardiovascular disease ● No history of pharmacologic or behavioral treatment (12 months duration or longer) by a specialty-trained physician (psychiatrist, neurologist, cardiologist) or mental health professional (e.g., social worker, clinical psychologist)
Exclusion Criteria		
● General medical condition, disease or neurological disorder that is likely to interfere with ability to complete assessments ● History of physical brain injury or blow to the head resulting in loss of consciousness greater than 10 min ● Severe impediment to vision, hearing and/or hand movement that is likely to interfere with ability to complete the assessments, or with comprehension of instructions or study requirements ● Pregnant or breastfeeding ● Any contraindication to being scanned in the 3.0T scanner (i.e., pacemaker or implanted device that has not been cleared for scanning) ● Lifetime history of psychosis or psychotic ideation ● Marijuana use in the past two weeks ● Substance or alcohol abuse within the past 12 months ● Presence of suicidal ideations representing imminent risk (defined as endorsement of specific suicidal plan or current intent) established by the MINI-Plus	● Currently taking any psychotropic medications for a mental health problem (i.e., SSRIs, benzodiazepines, etc.) ● Currently receiving therapy by a trained mental health professional (i.e., social worker, psychiatrist, clinical psychologist) for a mental health problem equivalent to 2+ formal sessions in the past month ● Current mania	

Abbreviations: MASQ, Mood and Anxiety Symptom Questionnaire; BAI, Beck Anxiety Inventory; RRS, Ruminative Responses Scale; BIS, Behavioral Inhibition Scale; MINI-Plus, MINI-International Neuropsychiatric Interview.

the four constructs identified using a factor analysis of data from (Grisanzio et al., 2018): anhedonia, anxious arousal, concentration, rumination, and tension. This survey will allow us to recruit a sample of participants presenting with clinically relevant symptoms. In order to be classified as a clinical participant, respondents will have to report that at least one symptom related statement "often" or "almost always/always" applied to them in the last two weeks and indicate that the symptoms caused significant distress and/or impairment. In order to be classified as a healthy control, respondents will have to report that symptom-related statements applied to them only "occasionally" or "rarely/never" in the last two weeks and indicate that any symptoms they may have experienced did not cause significant distress or impairment. Further, interested clinical and healthy control participants must not be taking any psychotropic medications for a mental health problem (i.e., SSRIs, benzodiazepines, etc.) or receiving therapy by a trained mental health professional (social worker, clinical psychologist, psychiatrist, etc.). This is to avoid confounding our results, since antidepressant treatment has been shown to affect brain function in our circuits of interest (Wessa and Lois, 2015). For participants who will be eligible and interested, a study coordinator will schedule an in-person visit to complete the baseline assessment.

4.3. Data collection at baseline visit

At the baseline in-person visit at Stanford, we will collect medical history and demographics, conduct two sessions of MRI, cognitive assessments, and self-report questionnaires. Refer to Table 2 for the full list of measures organized by RDoC construct. For additional self-reported and observer-rated measures that are supported by other funding, see Supplement. Every individual who participates in our study is given an extensive list of resources at the end of his/her visit, including: a list of mental health behavioral therapy services, online resources on how to find a therapist, a list of mutual help group treatments, a list of crisis hotlines, and information about our treatment studies that we are currently conducting in the lab. Moreover, every individual who completed our screening survey but is ineligible receives this same comprehensive list of resources. Since this could prompt people to start a treatment after the first visit, we closely ask about changes in treatment or significant lifestyle changes during our follow-up visits. We will then take this information into account when mapping different trajectories of disease in time. Additionally, we strictly adhere to a suicidality protocol that is implemented when we have reason to think that individuals are in danger of harming themselves or have current active suicidal thoughts, plans, or intentions. Trained medical doctors and/or clinical psychologists (who are current postdoctoral associates or faculty collaborators in the lab) are available for consultation and assist when clinical evaluation is warranted.

4.3.1. Medical history, diagnosis and demographics

At baseline, we will administer the Mini-International Neuropsychiatric Interview (MINI-Plus) to assess mood and anxiety disorders based on Diagnostic and Statistical Manual of Mental Disorders (DSM-5) and International Statistical Classification of Diseases and Related Health Problems (ICD-10) criteria (Sheehan et al., 1998). Diagnoses assessed will include: Persistent Depressive Disorder, Major Depressive Episode, Major Depressive Disorder, Major Depressive Disorder with Psychotic Features, Manic Episode, Hypomanic Episode, Bipolar I Disorder, Bipolar I Disorder with Psychotic Features, Bipolar II Disorder, Bipolar Disorder NOS, Panic Disorder, Agoraphobia, Social Anxiety Disorder, Obsessive Compulsive Disorder, Posttraumatic Stress Disorder, Psychotic Disorders, Mood Disorder with Psychotic Features, Anorexia Nervosa, Bulimia Nervosa, Binge-Eating Disorder, and Generalized Anxiety Disorder. Research personnel will also obtain comprehensive information about past and current medical history and additional sociodemographic data.

Table 2
Self-report and clinician-rated surveys, computerized cognitive tests of behavioral performance, and functional MRI paradigms organized by the RDoC subconstructs of interest and relevant neural circuits.

	Circuits	Behavior	Self-report	Paradigm
Negative valence systems				
Threat (acute/ potential)	Amygdala, hippocampus, insula, ACC, lateral PFC	Facial emotion identification	Anxiety	fMRI HCP-Emotion task, explicit emotion identification, implicit emotion priming, BAI,
Loss		Psychomotor speed, executive function performance	Depressed mood	BIS, MASQ-D30, PANAS
Positive valence systems				
Reward (responsiveness/ valuation)	Striatum, OFC, vmPFC, ACC	Positive emotion reactivity, reward responsiveness, reward learning	Anhedonia, lack of motivation	fMRI HCP-Gambling task, MASQ-D30, PANAS, BAS
Cognitive systems				
Working memory	DLPFC, DPC, precentral gyrus	Memory performance	Loss of memory	fMRI continuous performance task, picture sequence memory
Cognitive control		Concentration, impulsive behavior, speed of information processing, attention	Difficulties with concentration, reduced attention, lower productivity	Flanker, dimensional change card sort, picture vocabulary, list sorting, pattern comparison processing speed
Cross-cutting elements				
Default mode	PCC, AG, amPFC		Ruminations, inability to suppress negative thoughts	fMRI resting state, RRS, SOFAS, CQOL, Brief COPE

Abbreviations: ACC, Anterior Cingulate Cortex; PFC, Prefrontal Cortex; OFC, Orbitofrontal Cortex; vmPFC, Ventromedial Prefrontal Cortex; DLPFC, Dorsolateral Prefrontal Cortex; DPC, Dorsal Parietal Cortex; PCC, Posterior Cingulate Cortex; AG, Angular Gyrus; amPFC, Anterior Medial Prefrontal Cortex; HCP, Human Connectome Project; BAI, Beck Anxiety Inventory; BIS, Behavioral Inhibition Scale; MASQ-30, Mood and Anxiety Symptom Questionnaire; PANAS, Positive and Negative Affect Schedule; BAS, Behavioral Activation Scale; RRS, Ruminative Responses Scale; SOFAS, Social and Occupational Functioning Assessment Scale; CQOL, Current Quality of Life; Brief COPE, Brief Coping Orientation to Problems Experienced Inventory.

4.3.2. Brain imaging

The participant will undergo the following MRI scans, divided in 2 sessions with a break in between. 1) Spin-echo fieldmaps, 2) Resting state fMRI, 3) Emotion task fMRI, 4) Gambling task fMRI, 5) Selective working memory task fMRI, 6) T1-weighted anatomical, 7) T2-weighted anatomical 8) Spin-echo fieldmaps, 9) Resting state fMRI, 10) Diffusion-weighted imaging. Before the scan, a practice run of each task will be conducted on a computer outside of the scanner.

4.3.2.1. Negative valence systems. **"Emotion" Task:** This task from the HCP has been found to elicit robust amygdala and dorsolateral prefrontal activation (Barch et al., 2013; Hariri et al., 2002). Subjects are shown blocks of trials that either ask them to 1) determine which of the two faces (either angry or fearful expressions) presented on the bottom of the screen match the face at the top of the screen, or 2) determine which of the two shapes shown at the bottom of the screen match the shape at the top of the screen. There are 3 face blocks and 3 shape blocks, with 6 trials in each in which the stimulus is presented for 2 s with a 1 s intertrial interval (ITI). Each block is preceded by a 3 s task cue ("shape" or "face"), so that each block is 21 s long including the cue. Our contrast of interest for generalized linear model (GLM) analyses will be face blocks > shape blocks. One run of the task will be acquired in the first session, with posterior-anterior phase encoding direction.

4.3.2.2. Positive valence systems. **"Gambling" Task:** The HCP-DES adopts a version of the HCP gambling task modified to allow comparison of small and large gain and loss outcomes (Somerville et al., 2018). A question mark is displayed on the screen and the participant must guess whether a number is greater than or less than five (and indicate their answer via button presses). If the participant identifies correctly, they win money, and if they guess incorrectly, they lose money. At the end of the task, 5 trials are randomly selected and summed together to determine the participant's payment. Our contrast of interest for GLM analyses will be face reward > punishment trials. One run of the task will be acquired in the first session, with posterior-anterior phase encoding direction.

4.3.2.3. Cognitive systems. **"Continuous performance" Task:** This task has been used previously to probe working memory maintenance and sustained attention functions in depression (Korgaonkar et al., 2013). Participants are instructed to attend to yellow but not white letters and to press a button when the same yellow letter appears twice in a row. Stimuli are presented under three conditions: 30 sustained attention stimuli in which yellow letters appear twice in a row and participants respond to the consecutive yellow letter, 50 working memory stimuli in which yellow letters appear randomly and not consecutively and participants are required to maintain and update working memory without responding to the letters and 40 perceptual baseline stimuli in which to-be-ignored white letters are presented as a perceptual contrast to yellow letters. Working memory stimuli are not presented in a design that manipulates different levels of working memory demand. Our contrasts of interest for GLM analyses will be consecutive yellow letters > baseline, non-consecutive yellow letters > baseline and non-consecutive > consecutive letters. One run of the task is acquired in the first session, with posterior-anterior phase encoding direction.

4.3.2.4. Cross-cutting elements. **Resting State:** Participants will be instructed to stare at a white cross on a black background. During this time, their eyes will be monitored using an eye-tracker by the study coordinator to ensure that the participant is not asleep. Four separate 5-min runs of resting state data will be acquired, two with a posterior-anterior phase encoding direction and the other two with a posterior-anterior direction.

4.3.2.5. Acquisition details. Images will be acquired at the Stanford Center for Cognitive and Neurobiological Imaging (CNI) on a GE Discovery MR750 3T scanner using a Nova Medical 32-channel head coil. Two spin-echo fieldmaps will be acquired at the beginning of each session, one with a posterior-anterior phase encoding direction, the other with an anterior-posterior direction. All fMRI scans will be conducted using a blipped-CAIPI simultaneous multislice "multiband" acquisition (Setsompop et al., 2012). A separate single-band scan is acquired before each of the multiband acquisitions to provide calibration data for the parallel image reconstruction which uses the split-slice-GRAPPA method (Cauley et al., 2014).

1. **Spin-echo fieldmaps**: TE = 55.5 ms, TR = 6 s, FA = 90, acquisition time = 18 s, field of view = 220.8 × 220.8 mm, 3D matrix size = 92 × 92 × 60, slice orientation = axial, angulation to anterior commissure - posterior commissure (AC-PC) line, phase encoding = AP and PA,

receiver bandwidth = 250 kHz, readout duration = 49.14 ms, echo spacing = 0.54 ms, voxel size = 2.4 mm isotropic.

2. **Single-band calibration**: TE = 30 ms, TR = 4.4 s, FA = 90, acquisition time = 13 s, field of view = 220.8 × 220.8 mm, 3D matrix size = 92 × 92 × 60, slice orientation = axial, angulation to AC-PC line, phase encoding = PA, receiver bandwidth = 250 kHz, readout duration = 49.14 ms, echo spacing = 0.54 ms, number of volumes = 4, voxel size = 2.4 mm isotropic.
3. **Multiband fMRI**: TE = 30 ms, TR = 0.71 s, FA = 54, acquisition time = 5:12 (rest), 2:25 (emotion task), 3:44 (gambling task), 5:08 (continuous performance task), field of view = 220.8 × 220.8 mm, 3D matrix size = 92 × 92 × 60, slice orientation = axial, angulation to AC-PC line, phase encoding = PA, receiver bandwidth = 250 kHz, readout duration = 49.14 ms, echo spacing = 0.54 ms, number of volumes = rest = 440, emotion = 204, gambling = 316, CPT = 434, multiband factor = 6, calibration volumes = 2, voxel size = 2.4 mm isotropic. Compared to HCP-HYA parameters, this sequence had lower multiband factor (6 versus 8) and larger voxel size (2.4 versus 2) to increase the signal to noise ratio, especially in our subcortical structures of interest.
4. **T1-weighted**: TE = 3.548 ms, MPRAGE TR = 2.84s, FA = 8, acquisition time = 8:33, field of view = 256 × 256 mm, 3D matrix size = 320 × 320 × 230, slice orientation = sagittal, angulation to AC-PC line, receiver bandwidth = 31.25 kHz, fat suppression = no, motion correction = PROMO, voxel size = 0.8 mm isotropic.
5. **T2-weighted**: TE = 74.4 ms, TR = 2.5 s, FA = 90, acquisition time = 5:42, field of view = 240 × 240 mm, 3D matrix size = 320 × 320 × 216, slice orientation = sagittal, angulation to AC-PC line, receiver bandwidth = 125 kHz, fat suppression = no, motion correction = PROMO, voxel size = 0.8 mm isotropic.
6. **Diffusion-weighted**: A total of 4 acquisitions, TE = 80 ms, TR = 3.2 s, FA = 77, acquisition time = 4:48, field of view = 210 × 210 mm, 3D matrix size = 140 × 140 × 84, slice orientation = axial, angulation to AC-PC line, phase encoding = AP and PA, receiver bandwidth = 125 kHz, readout duration = 113.12 ms, echo spacing = 0.808 ms, directions = 74, 74, 76, 76, b-values = 1500, 3000, number of b0 = 5, 5, 5, 5, multi-shell, equal spacing, single spin echo, cardiac gating = no, calibration volumes = 2, voxel size = 1.5 mm isotropic.

4.3.3. Computerized tests of behavioral performance

4.3.3.1. WebNeuro tasks. These tasks will be executed on a desktop computer by the participant and described in detail in (Silverstein et al., 2007; Watters and Williams, 2011). The software used to run the tasks includes standardized task instructions. Psychometric properties have been established for each of these tests, including norms, construct validation, validation against traditional neuropsychological tests tapping equivalent functions, test-retest reliability, and consistency across cultures (Williams et al., 2016). For each test, we will record accuracy and reaction time.

4.3.3.1.1. Positive and negative valence systems.

1. **Explicit emotion identification:** Participants identify the emotion of 96 facial expressions (neutral, happy, sad, fear, anger, or disgust).
2. **Implicit emotion priming:** 24 of the photographs from the explicit emotion identification task are randomly selected for each participant and are presented a second time. Each will be shown beside one of 24 new photographs showing a different individual but of the same sex and emotion. For each pairing, participants indicate which of the two faces they have seen in the previous task.

4.3.3.1.2. Cognitive systems.

1. **Continuous performance test:** A series of 125 similar looking letters are presented to the participant on the computer screen. If the same letter appears twice in a row, the participant required to press the spacebar.

4.3.3.2. NIH toolbox tasks. These behavioral tasks are executed on an iPad with the study coordinator and described in detail in (Weintraub et al., 2013).

4.3.3.2.1. Cognitive systems.

1. **Flanker Inhibitory Control and Attention Test:** A measure of executive function. This task requires the participant to focus on a particular stimulus while inhibiting attention to the stimuli flanking it (40 trials).
2. **Dimensional Change Card Sort Test:** A measure of executive function, specifically cognitive flexibility and attention. Two target pictures are presented that vary along two dimensions (e.g., shape and color). Subjects are asked the match a series of bivalent test pictures (e.g., yellow balls and blue trucks) to the target pictures, first according to one dimension (e.g., color) and then, after a number of trials, according to the other dimension (e.g., shape) (40 trials).
3. **Picture Sequence Memory Test (Form A):** A measure of episodic memory, whereby sequences of pictured objects and activities are presented in a specific order, and the participant is asked to reproduce the sequence of pictures that is shown on the screen.
4. **Picture Vocabulary Test:** A measure of receptive vocabulary administered in a computer-adaptive test (CAT) format. The task is to pick a picture that best matches a spoken word.
5. **List Sorting Working Memory Test:** A measure of working memory. This task requires the participant to recall and sequence different visually and orally presented stimuli. Pictures of different foods and animals are displayed with both an accompanying audio recording and written text that name the item. The participant is asked to say the items back to the study coordinator in size order from smallest to largest.
6. **Pattern Comparison Processing Speed Test:** A measure of processing speed. This task requires participants to discern whether two side-by-side pictures are the same or not (130 items).

4.3.4. Self-report measures

The majority of our self-report measures are presented in a computerized format using the REDCap database. Scores for individual items are recorded and then summed automatically according to symptom cluster and scale definitions. An exception to automated scoring is the SOFAS, which is rated by study coordinators.

4.3.4.1. Negative and positive valence systems.

1. **Beck Anxiety Inventory (BAI):** A 21-item self-report inventory for measuring the severity of common symptoms of anxiety that the participant has had during the past week, such as numbness and tingling, sweating not due to heat, and fear of the worst happening (Beck et al., 1988).

2. **Behavioral Inhibition Scale (BIS):** A 7-item scale assessing behavioral inhibition (i.e., concern over and reactivity to aversive events) on a 4-point scale ranging from 1 to 4 (Carver and White, 1994).

3. **Mood and Anxiety Symptom Questionnaire short form (MASQ-D30):** A 30-item questionnaire based on the Tripartite Model of Anxiety and Mood that provides scores in three domains: General Distress, Anhedonic Depression, and Anxious Arousal. The questions refer to how the subject has been feeling in the past two weeks (Wardenaar et al., 2010).

4. **Positive and Negative Affect Schedule (PANAS):** A 20-item questionnaire that measures positive and negative affect on a 5-point scale ranging from 1 to 5 (Watson et al., 1988).

5. **Behavioral Activation System Scale (BAS):** A 13-item scale assessing behavioral activation (i.e., reward responsiveness, drive,

and fun seeking) on a 4-point scale ranging from 1 to 4 (Carver and White, 1994).

4.3.4.2. Cross-cutting elements.

1. **Ruminative Responses Scale (RRS):** A 22-item self-report questionnaire that assesses two aspects of rumination; brooding and reflecting pondering. It is scored on a 4-point scale ranging from 1 to 4 (Parola et al., 2017).

2. **Social and Occupational Functioning Assessment Scale (SOFAS):** The SOFAS is a derivative of the Global Adjustment Scale and reflects the individual's level of social and occupational functioning, rated by a study coordinator on a scale between 0 and 10 (Morosini et al., 2000).

3. **Current Quality of Life (CQOL):** A measure of an individual's general mental and physical health during the previous 30 days (Burckhardt and Anderson, 2003). Available in the Phenotypes and eXposures (PhenX) Toolkit (C. M. Hamilton et al., 2011a).

4. **Brief Coping Orientation to Problems Experienced Inventory (Brief COPE)**: A 28-item questionnaire assessing usage of various coping strategies (Carver, 1997). Available in the PhenX Toolkit (C. M. Hamilton et al., 2011).

4.4. Follow-up outcome measures

Every 3 months for one year after the in-person baseline visit (4 times total), clinical participants will complete a 10–15 min online questionnaire regarding symptoms, treatments, and life events. The PHQ-9, GAD-7, and SWLS are also included. In addition, one year after the baseline assessment, clinical participants will complete a diagnostic interview over the telephone (MINI-Plus) and cognitive testing remotely (WebNeuro).

4.5. Data management and access

Neuroimaging data will be managed using the quality control and data management infrastructure Flywheel (https://flywheel.io/) at the Stanford CNI. For the computerized behavioral tests, the computer will register each response and collects these with time stamps to a log file. For the questionnaires, each self-reported response entered by participants will be logged. These data are stored in a protected health information (PHI)-protected database (REDCap) and then integrated with the neuroimaging data.

As one of the "Human Connectome Studies Related to Human Disease", all the data will ultimately be shared openly via the Human Connectome Project database (https://db.humanconnectome.org). Neuroimaging and behavioral data will be downloaded from Flywheel and then reuploaded to the Connectome Coordinating Facility in batches ranging from 17 to 50 subjects quarterly throughout the period of data acquisition. Data will be released in the second quarter of 2022. Similarly to all other Connectomes Related to Human Disease projects, The Connectome Coordinating Facility will run the same processing pipeline previously run on the HCP-HYA release and the upcoming HCP Lifespan. In summary, this pipeline includes: structural, functional, multi-Run ICAFIX, MSM-All and diffusion preprocessing as well as task analysis where applicable (Glasser et al., 2013; Harms et al., 2018). They will then distribute the raw and preprocessed image files for all imaging modalities. Quality controls will be performed at the Connectome Coordinating Facility following a set of best practices developed internally and available for consultation to study Investigators.

5. Quality control

In the following sections we present an overview of the imaging data from a representative sample of 29 healthy control participants from HCP-DES (13 females, mean age = 28.19 ± 4.85, min: 21, max: 35). Preprocessing of structural, functional and diffusion data was conducted with the minimal preprocessing HCP pipelines version 3.27.0 (Glasser et al., 2013). This preprocessing includes cortical and subcortical segmentation of structural images, realignment, EPI distortion correction and surface-based registration of functional data, and mapping of all data to grayordinate space. For diffusion data, this also includes eddy current, motion and susceptibility distortion correction. The HCP-DES takes advantage of its high-resolution multimodal structural scans to perform registration to grayordinate space and file conversion to the CIFTI format. This allows combined cortical surface and subcortical volume analyses. We expect the adoption of CIFTI to boost the power of functional analyses and improve comparisons across participants.

5.1. Resting state

Resting state functional data had good signal-to-noise ratio (SNR; grayordinate mean = 85.34 ± 38.42). We used MELODIC (Multivariate Exploratory Linear Decomposition into Independent Components) version 3.15, part of FSL (FMRIB's Software Library, www.fmrib.ox.ac.uk/fsl). The following pre-processing was applied to the input data: masking of non-brain voxels; voxel-wise de-meaning of the data; normalisation of the voxel-wise variance. Pre-processed data were whitened and projected into a 25-dimensional subspace using Principal Component Analysis. The whitened observations were decomposed into sets of vectors which describe signal variation across the temporal domain (time-courses), the session/subject domain and across the spatial domain (maps) by optimizing for non-Gaussian spatial source distributions using a fixed-point iteration technique (Hyvärinen, 1999). Estimated Component maps were divided by the standard deviation of the residual noise and thresholded by fitting a mixture model to the histogram of intensity values (Beckmann and Smith, 2004). MELODIC successfully identified well-established networks, such as the default mode, salience, visual and motor (Fig. 3).

5.2. Emotion

The Emotion task had good SNR (grayordinate mean = 99.53 ± 50.06). Subject-level analysis was conducted using the HCP pipelines and was entirely constrained to grayordinates. In summary, a 2 mm smoothing was applied and a GLM analysis was run using FSL FEAT (Woolrich et al., 2001) including as regressors the Faces and Shapes blocks of the task, each convolved with a double-gamma hemodynamic function and their first order temporal derivatives. The contrast Faces > Shapes was then analyzed at the group level using FSL PALM (Winkler et al., 2014). To account for the topological differences of cortical and subcortical components of the CIFTI dense file, inference from both representations was computed separately by using 10,000 permutations with sign-flipping. Results were considered significant when Bonferroni corrected $p < 0.05$ at the cluster level. Matching of faces versus shapes showed significant activations in the bilateral dorsolateral prefrontal and occipital cortices, in the fusiform gyrus and in the amygdalae (Fig. 4).

5.3. Gambling

The Gambling task had good SNR (grayordinate mean = 93.86 ± 35.31). Analysis of this task was conducted as reported above, with the two events of interest being win and loss trials. The contrast Win > Loss was then analyzed at the group level. The win of money versus loss showed significant activations in the bilateral dorsolateral prefrontal, parietal and occipital cortices, and in the striatum (Fig. 5).

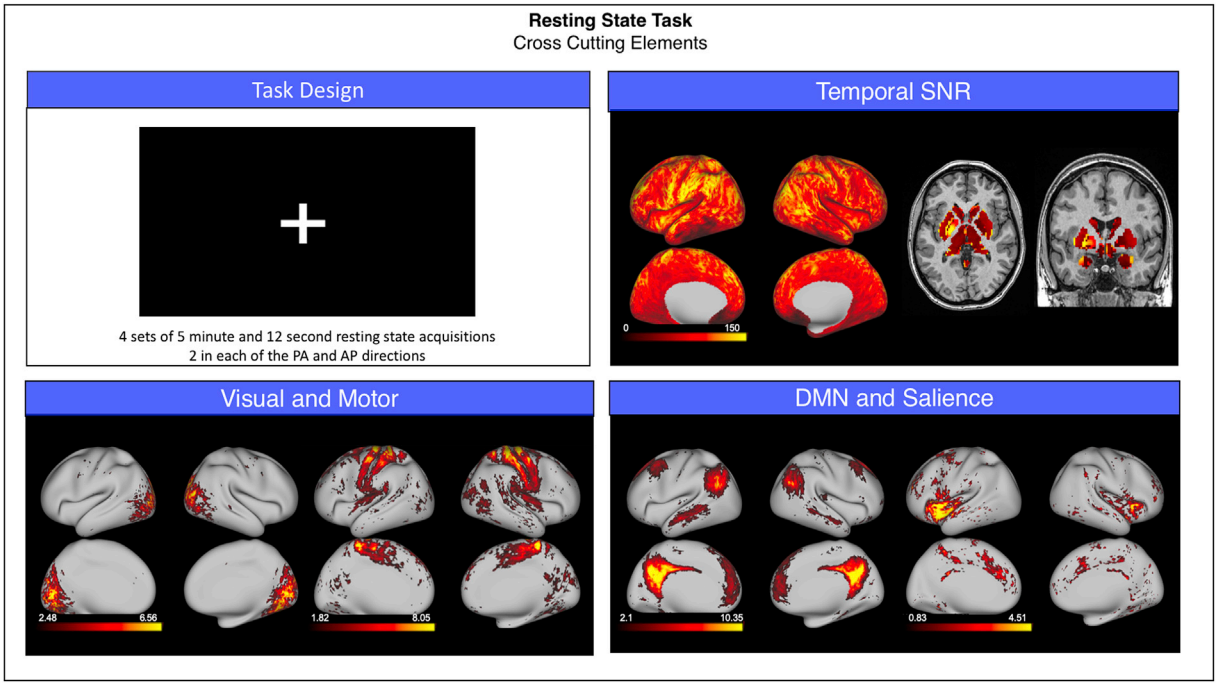

Fig. 3. Summary of representative functional results for the resting state scan. We show a diagram summarizing task design (top left), greyordinate-wise temporal SNR (top right) and the spatial weights (z-scores) for four canonical functional networks identified by independent component analysis (bottom left and bottom right). *Abbreviations*: PA = posterior-anterior phase encoding; AP = anterior-posterior phase encoding; SNR = signal to noise ratio; DMN = default mode network.

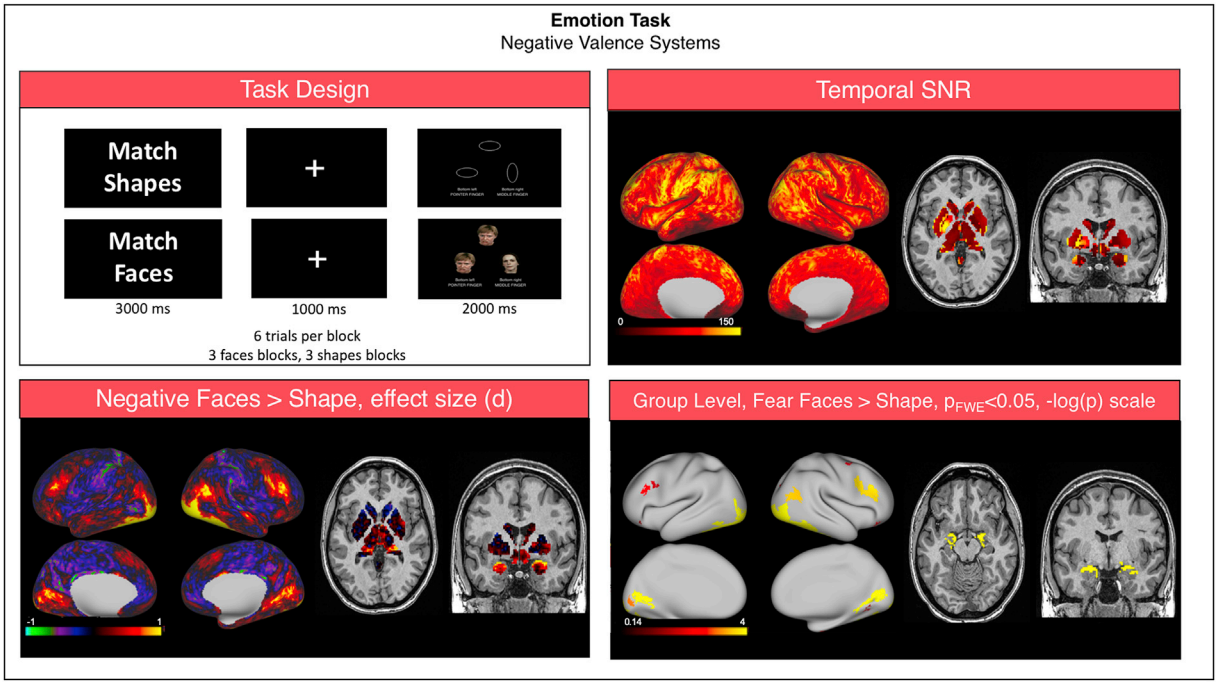

Fig. 4. Summary of representative functional results for the "Emotion" task. We show a diagram summarizing task design (top left), greyordinate-wise temporal SNR (top right). For the Negative Faces > Shapes contrast at the group level we show the effect size (Cohen d, bottom left) and significant activations (bottom right). *Abbreviations*: SNR = signal to noise ratio; FWE = family-wise error correction.

5.4. Continuous performance

The continuous performance task had good SNR (grayordinate mean = 92.59 ± 45.66). Analysis of this task was conducted as reported above, with the two modeled events being the consecutive and non-consecutive yellow letters. The contrast consecutive letters > Baseline was then analyzed at the group level. The recognition of a target letter was associated with significant activation in the bilateral dorsolateral prefrontal, parietal, motor, temporal and insular cortices, and in the striatum and cerebellum (Fig. 6).

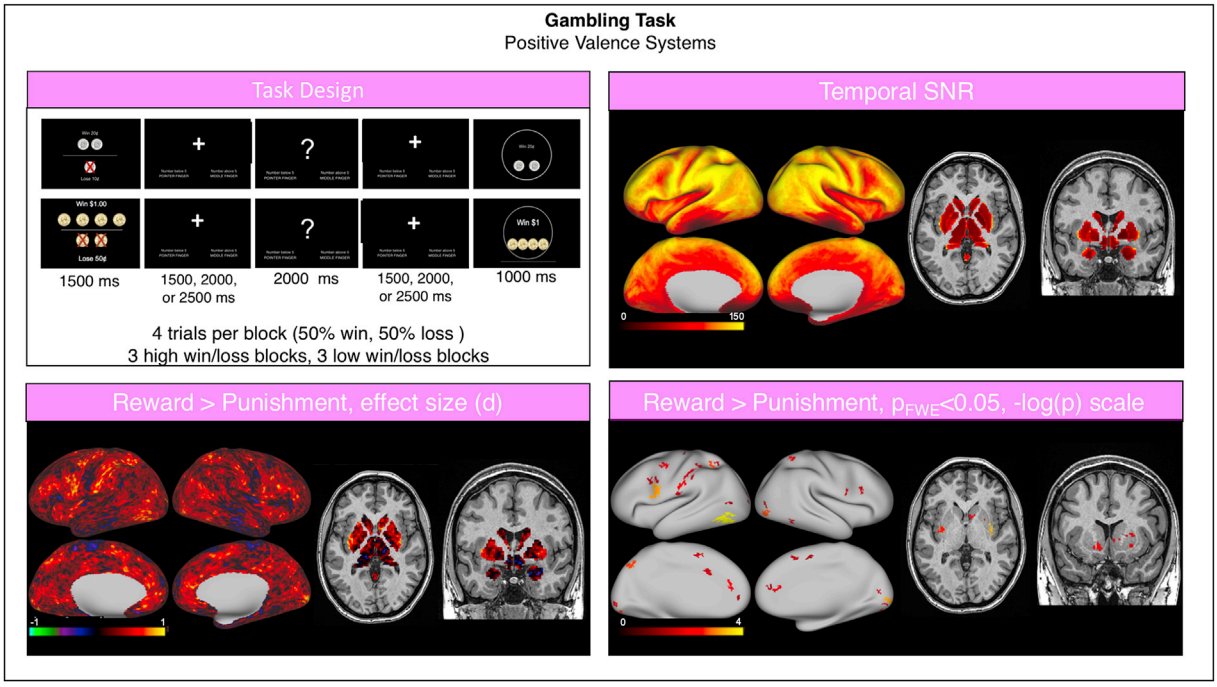

Fig. 5. Summary of representative functional results for the "Gambling" task. We show a diagram summarizing task design (top left), greyordinate-wise temporal SNR (top right). For the Reward > Punishment contrast at the group level we show the effect size (Cohen d, bottom left) and significant activations (bottom right). Abbreviations: SNR = signal to noise ratio; FWE = family-wise error correction.

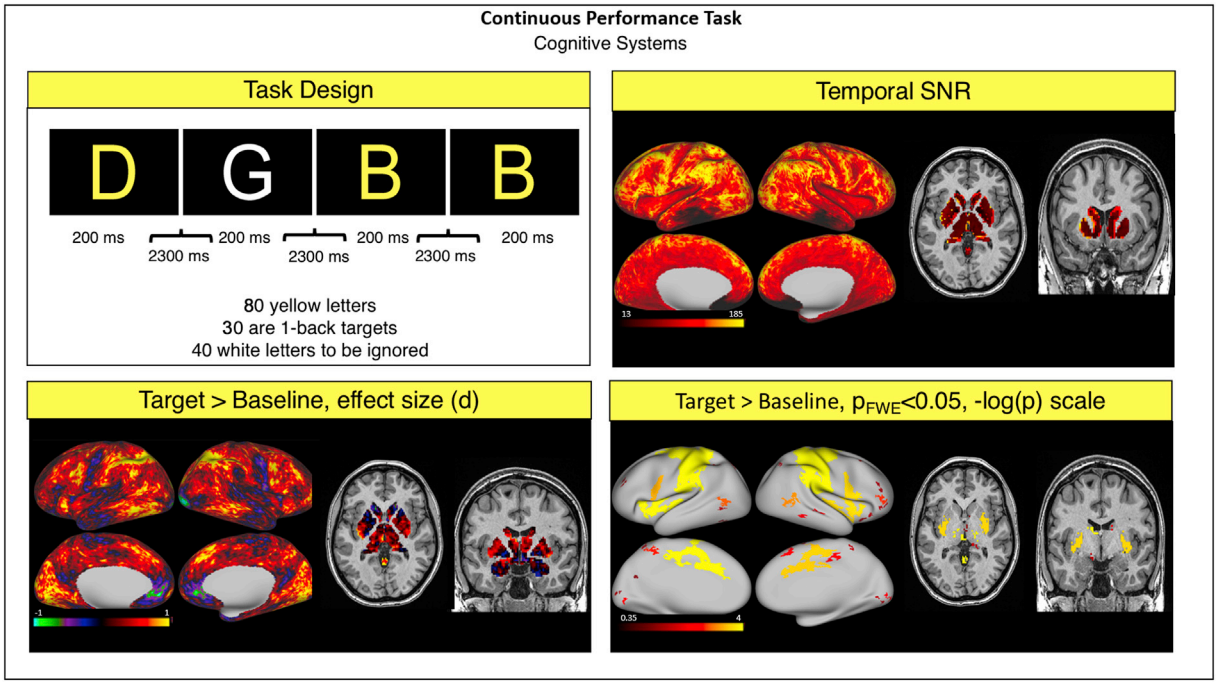

Fig. 6. Summary of representative functional results for the "Continuous Performance" Task. We show a diagram summarizing task design (top left), greyordinate-wise temporal SNR (top right). For the Target > Baseline contrast at the group level we show the effect size (Cohen d, bottom left) and significant activations (bottom right).
Abbreviations: SNR = signal to noise ratio; FWE = family-wise error correction.

5.5. Diffusion

For 5 subjects, diffusion data could not be collected, so in the remaining 24 participants (12 females, mean age = 28.31, min: 21.39, max: 35.90), we quantified fractional anisotropy (FA) of established white matter tracts (for the b = 1500 s/mm^2 shell) by using Reproducible Tract Profiles (Lerma-Usabiaga et al., 2019b). Briefly, this pipeline performed constrained spherical deconvolution modeling on the

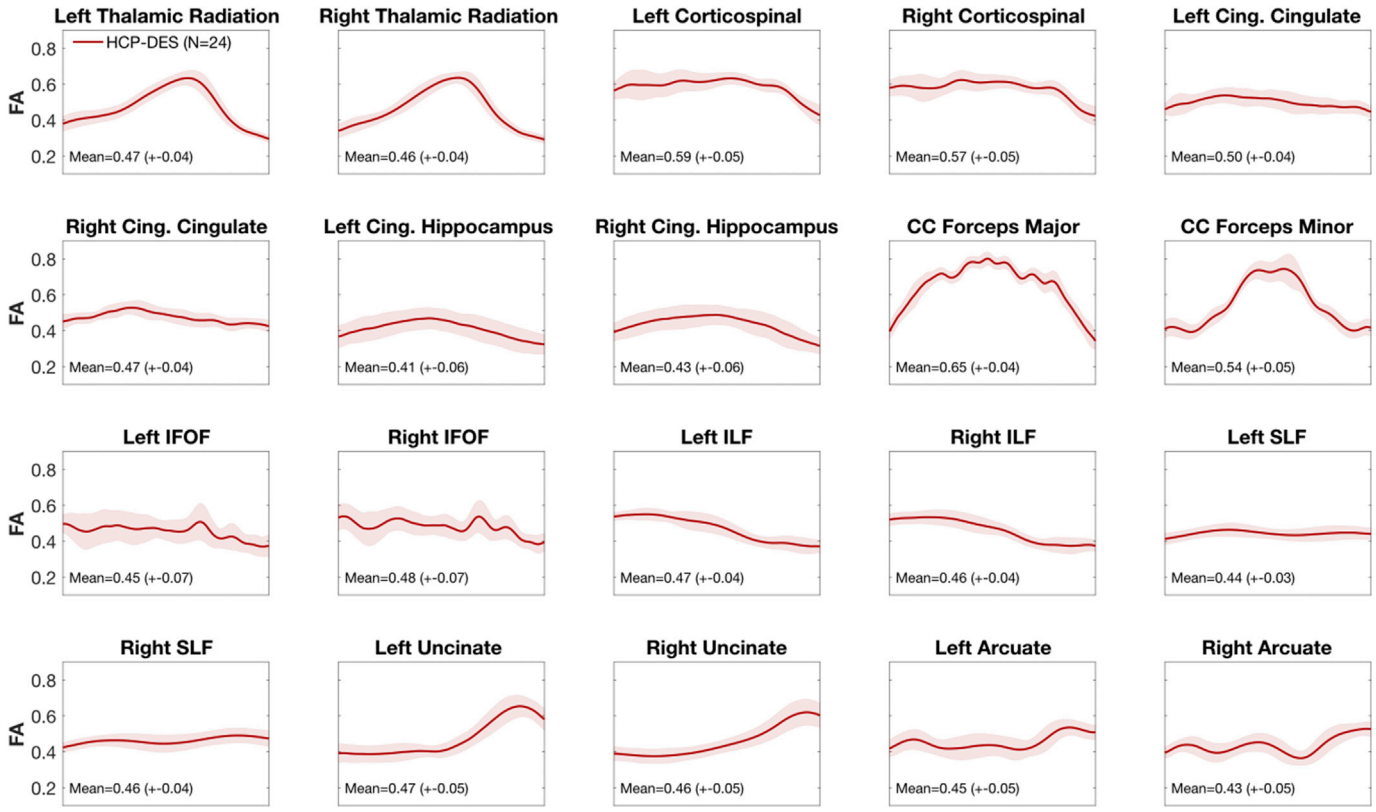

Fig. 7. doFractional anisotropy along white matter fiber tracts in our representative sample. Using reproducible tract profiles (Lerma-Usabiaga et al., 2019b), we show the group level mean (red line) and SD (shaded area) of FA at 100 equally spaced intervals along 10 tracts (left and right).
Abbreviations: CC = corpus callosum; Cing. = cingulum, FA = fractional anisotropy; FOF = fronto-occipital fasciculus; HCP-DES = human connectome project for disordered emotional states; ILF = inferior longitudinal fasciculus; SLF = superior longitudinal fasciculus; SD = standard deviation.

preprocessed diffusion data using both b = 1500 and 3000 s/mm^2 shells (Tournier et al., 2019), followed by whole brain white matter streamlines estimation using ensemble tractography and linear fascicle evaluation (Pestilli et al., 2014; Takemura et al., 2016). Then, a modified version of automated fiber quantification (Yeatman et al., 2012) was used to segment streamlines into tracts based on regions of interest. Mean FA varied between 0.43 and 0.65, with a SD across subjects between 0.03 and 0.07, depending on the tract. Profiles of FA along the tract were consistent between subjects (Fig. 7).

6. Comparison with available HCP data

In the following section we compare imaging data from the sample outlined above with data from a matched sample of 29 healthy controls from the HCP Healthy Young Adult (HYA) data release (13 females, mean age = 27.72 ± 4.57, min: 22, max: 36). This data was collected on a custom Siemens Skyra "Connectom" scanner (see Barch et al., 2013; Van Essen et al., 2013 for full protocol details), preprocessed with the HCP pipelines and made openly available through ConnectomeDB (https://db.humanconnectome.org/). After downloading the data, we repeated the steps outlined in the previous section to compare the HCP-HYA and HCP-DES datasets. Our goal was to provide a preliminary outlook on the generalizability of findings from one dataset to the other, given that, despite all efforts undertaken to minimize discrepancies, they were acquired on different scanners, at different sites and with different protocols. Concerning behavior and self-reports, Supplementary Table 2 draws a comparison between each of the measures collected in HCP-DES and corresponding measures released in the HCP-HYA dataset. Given the differences in the aims and target populations between the two datasets, the same exact questionnaires and tests were not always used. However, in this table we suggest which measurements from the HCP Healthy Young Adult overlap in terms of domains and contain similar items to the ones we use in HCP-DES.

6.1. Resting state

Compared to HCP-HYA, resting state functional data from HCP-DES had higher SNR (grayordinate mean = 99.53 ± 50.06 and 49.10 ± 25.85 respectively). In both datasets, MELODIC identified well-established networks with comparable characteristics, such as the default mode network (Fig. 8).

6.2. Emotion

Compared to HCP-HYA, "Emotion" task functional data from HCP-DES had higher SNR (grayordinate mean = 85.34 ± 38.42 and 56.51 ± 26.74 respectively). In both datasets, matching of faces versus shapes showed significant activations in the bilateral dorsolateral prefrontal and occipital cortices, in the fusiform gyrus and in the amygdalae (Fig. 9).

6.3. Gambling

Compared to HCP-HYA, "Gambling" task functional data from HCP-DES had higher SNR (grayordinate mean = 93.86 ± 35.31 and 56.38

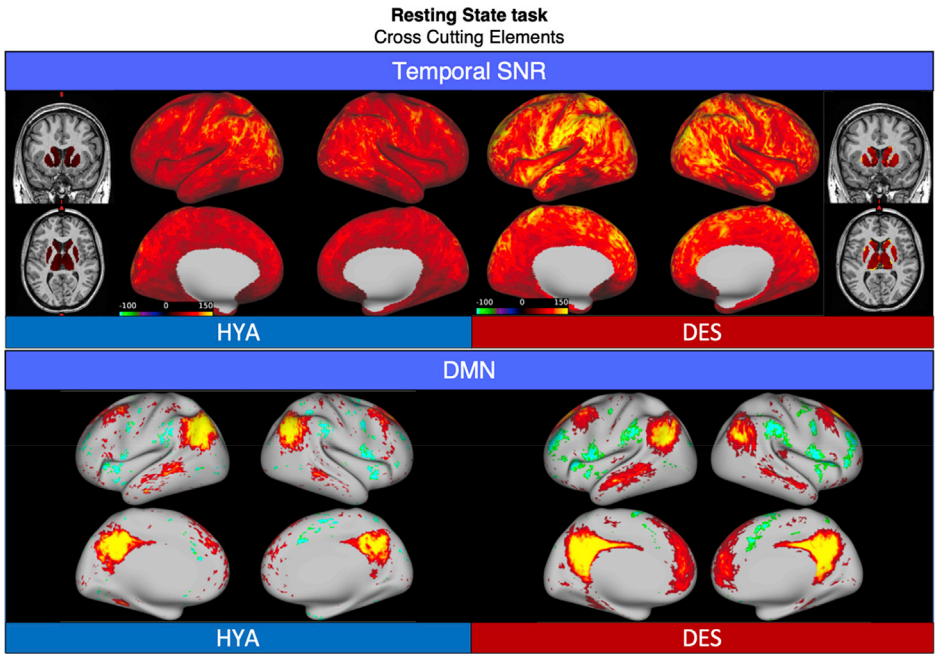

Fig. 8. Comparison of representative functional results for the resting state scan between HYA and DES. We show a diagram summarizing greyordinate-wise temporal SNR (top) and the spatial weights (z-scores) for the default mode network identified by independent component analysis (bottom).
Abbreviations: HYA = healthy young adult data release; DES = human connectome project for disordered emotional states; SNR = signal to noise ratio; DMN = default mode network.

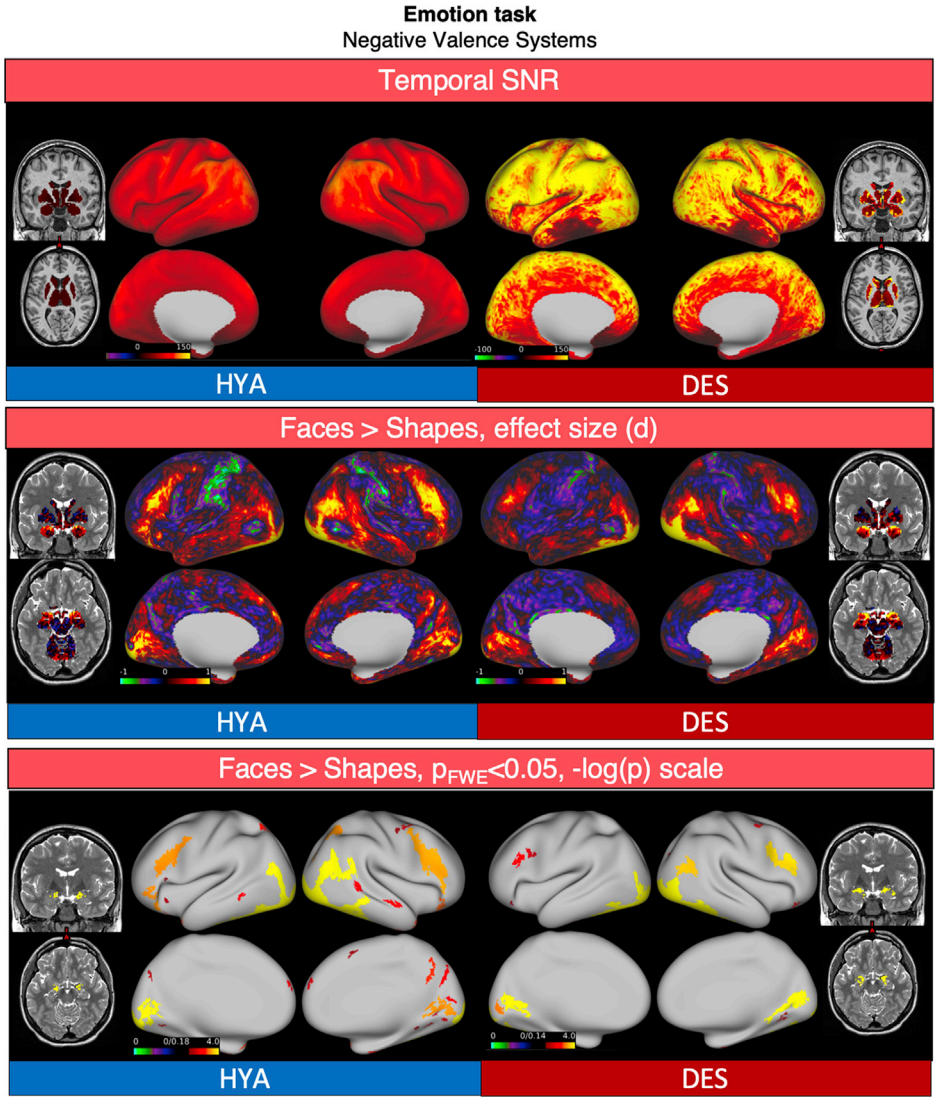

Fig. 9. Comparison of representative functional results for the "Emotion" task between HYA and DES. We show a diagram summarizing greyordinate-wise temporal SNR (top). For the Negative Faces > Shapes contrast at the group level we show the effect size (Cohen d, middle) and significant activations (bottom).
Abbreviations: HYA = healthy young adult data release; DES = human connectome project for disordered emotional states; SNR = signal to noise ratio; FWE = family-wise error correction.

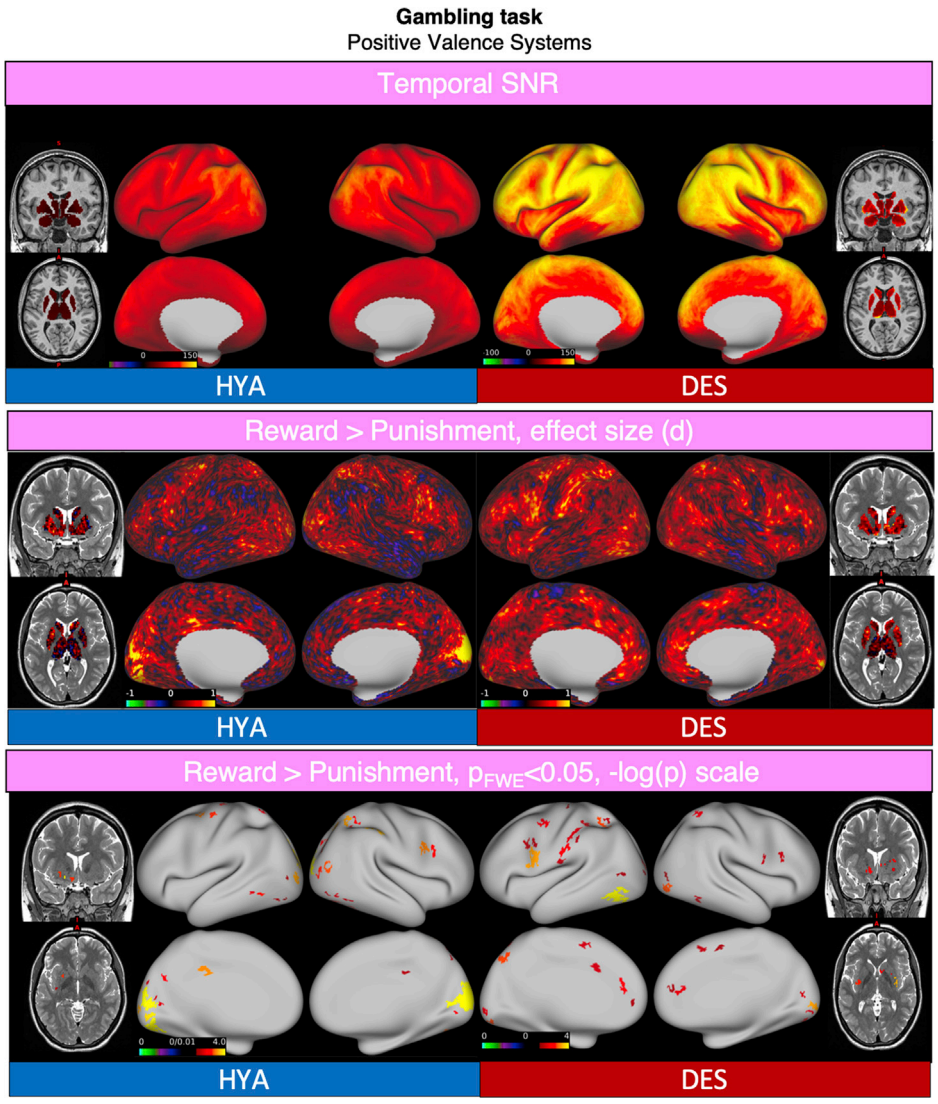

Fig. 10. Comparison of representative functional results for the "Gambling" task between HYA and DES. We show a diagram summarizing greyordinate-wise temporal SNR (top). For the Reward > Punishment contrast at the group level we show the effect size (Cohen d, middle) and significant activations (bottom).
Abbreviations: HYA = healthy young adult data release; DES = human connectome project for disordered emotional states; SNR = signal to noise ratio; FWE = family-wise error correction.

± 27.33 respectively). In both datasets, win of money versus loss showed significant activations in the bilateral dorsolateral prefrontal, parietal and occipital cortices, and in the striatum (Fig. 10).

6.4. Continuous performance

As a comparison for the HCP-DES "Continuous Performance" task, we chose the HCP-HYA "Working Memory" task since both were designed to engage the construct of working memory. To quantify task activations, we chose to focus on the 0-back condition of this task. In this condition, participants were shown a stimulus at the beginning of a task block and were instructed to press a button every time the stimulus was presented. We compare this condition to the button press in response to two consecutive yellow letters in HCP-DES.

Data from HCP-DES had higher SNR (grayordinate mean = 92.59 ± 45.66 and 54.24 ± 26.20 respectively).

In both datasets, the recognition of the target stimulus was associated with significant activation in the bilateral dorsolateral prefrontal, parietal, motor, temporal and insular cortices, and in the striatum and cerebellum (Fig. 11).

6.5. Diffusion

Tract profiles and standard deviations of FA measurements along the tract were comparable between the HCP-DES and HCP-HYA datasets. Mean FA was consistently higher for the HCP-HYA dataset, because of the different b-values used in the acquisition/FA calculation (1000 s/mm^2 for HCP-HYA compared to 1500 s/mm^2 for HCP-DES) (Lerma-Usabiaga et al., 2019a) (Fig. 12).

7. Intended use and limitations

The current prevalent framework in psychiatry relies on symptoms to formulate categorical diagnoses. In contrast, the HCP-DES will contribute to a novel, dimensional taxonomy informed by systems neuroscience through the multimodal quantification of the brain networks that underlie disordered emotional states. Measuring brain connectivity, behavior and clinical symptoms will permit us to examine the relations among these units of analysis and to predict outcomes relevant to disability and burden of illness over one year. Finally, this transdiagnostic approach to emotional disorders will allow us to develop data-driven, machine-learning methods to elucidate how disruption in the negative valence, positive valence and cognitive systems combine to form naturally organized clusters of patients.

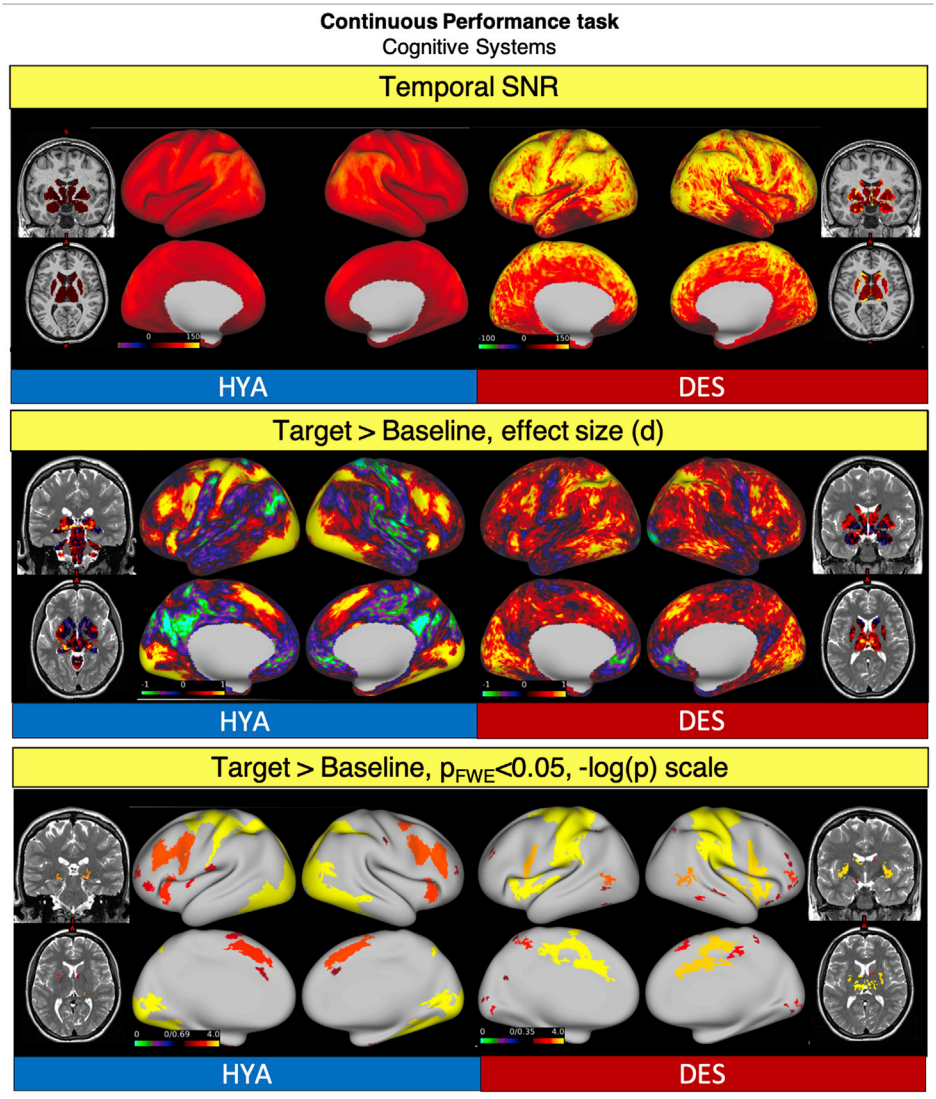

Fig. 11. Comparison of representative functional results for the "Working Memory" HYA task and the "Continuous Performance" DES task. We show a diagram summarizing greyordinate-wise temporal SNR (top). For the Target Stimulus > Baseline contrast at the group level we show the effect size (Cohen d, middle) and significant activations (bottom).
Abbreviations: HYA = healthy young adult data release; DES = human connectome project for disordered emotional states; SNR = signal to noise ratio; FWE = family-wise error correction.

Data collected by the HCP-DES will also be made publicly available through the Connectome Coordinating Facility. The multimodal nature of the HCP-DES imaging will help answer basic scientific questions concerning the relations between structural and functional connectomes in mood disorders. Of particular interest to multi-site collaborations, measures collected in HCP-DES show a substantial overlap with those in other HCP datasets. Therefore, the data will contribute to efforts to quantify the naturally occurring heterogeneity in brain connectivity across normative and clinical populations.

While this project offers a number of advances in characterizing emotional disorders, it is important to consider the limitations that restrict its scope and generalizability. In the HCP-DES, participants on psychiatric medication will be excluded in order to examine patterns of brain connectivity without the effect of medication. Thus, the HCP-DES will be most suited to make inferences about brain changes which might be different from the ones of patients currently receiving treatment.

Additionally, we anticipate technical challenges in merging data from the HCP-DES project with other projects that acquired brain imaging data on a different model of scanner with some important differences in the scanning protocol. Concerning the harmonization of the data collected by HCP-DES within the HCP consortium, first of all it is important to note that three other HCP Connectomes Related to Human Disease are currently investigating other aspects of mood disorders: anxious misery, major depression in teenagers and predictors of treatment response to fast-acting therapies (see https://www.humanconnectome.org/disease-studies). These other studies target a similar population to HCP-DES and are acquiring data on Siemens scanners similar to the Skyra "Connectom". Therefore, they will provide another useful benchmark to test generalizability of findings or to run meta- and mega-analyses across sites collecting similar measures (e.g. questionnaires of symptom severity). For merging of these datasets, recently developed algorithms to correct for site effects will likely be needed (see for example COMBAT, (Fortin et al., 2017; Johnson et al., 2007). However, it is important to highlight that besides technical challenges, collection of data at different sites also allows to explore how findings generalize across device vendors and populations. In this respect, our preliminary data show that overlapping task activations and comparable resting state networks as well as tract profiles can be detected from the data collected on the HCP-DES GE Discovery scanner and the Central Connectome Facility Siemens Skyra "Connectom". Interestingly, temporal SNR was generally higher in HCP-DES especially in subcortical structures, potentially due to a lower

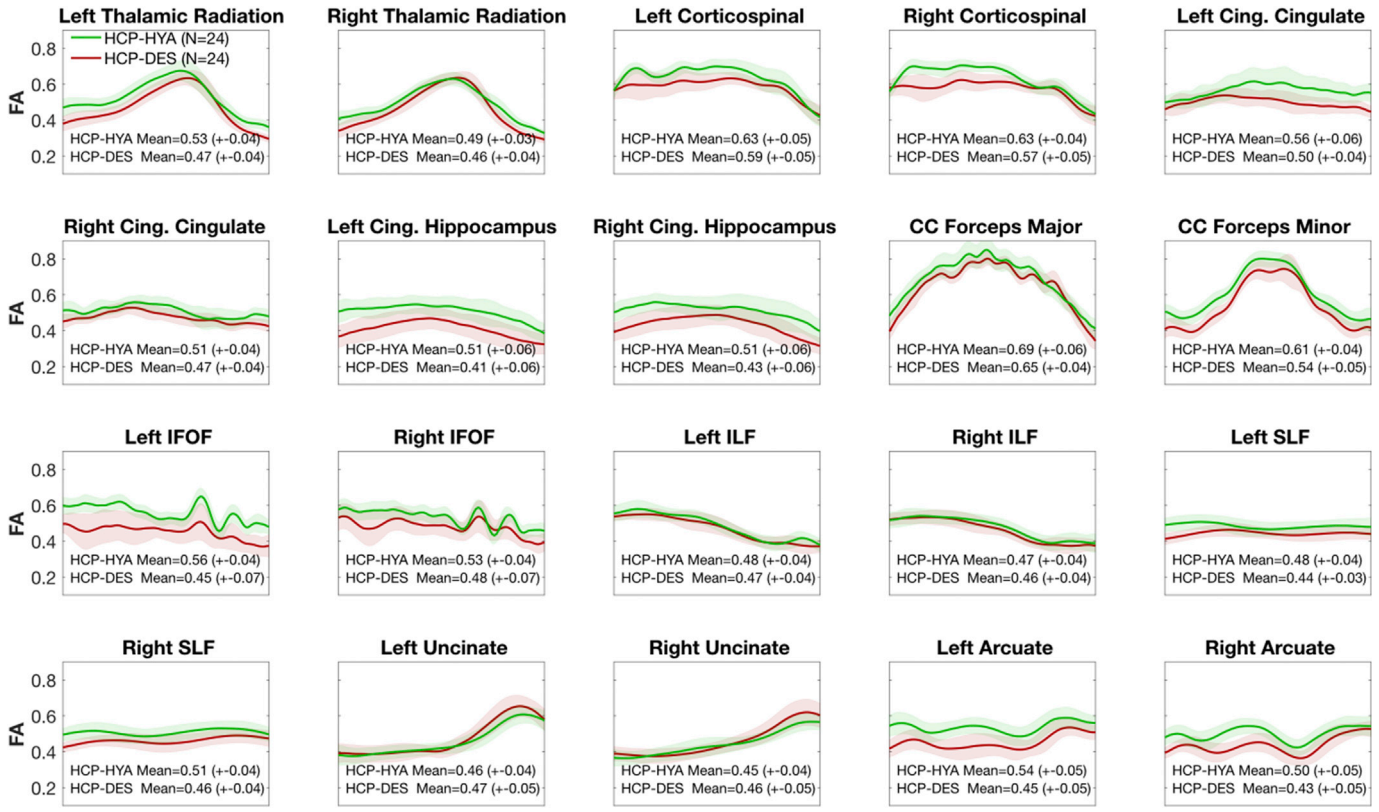

Fig. 12. Comparison of fractional anisotropy along white matter fiber between the HCP-DES and HCP-HYA datasets. Using reproducible tract profiles (Lerma-Usabiaga et al., 2019b), we show the group level mean (red = HCP-DES, green = HCP-HYA) and SD (shaded area) of FA at 100 equally spaced intervals along 10 tracts (left and right).

Abbreviations: CC = corpus callosum; Cing. = cingulum, HCP-HYA = healthy young adult data release; HCP-DES = human connectome project for disordered emotional states, FA = fractional anisotropy; FOF = fronto-occipital fasciculus; ILF = inferior longitudinal fasciculus; SLF = superior longitudinal fasciculus; SD = standard deviation.

multiband acquisition factor (6 compared to 8 in HCP-HYA).

To conclude, in the Human Connectome Project for Disordered Emotional States we will obtain cutting-edge multimodal imaging, self-reports and behavioral measures in a rich dataset that will be made publicly available. This project is designed to assess how brain circuits relevant to the RDoC domains of negative valence, positive valence, cognitive systems and cross-cutting elements are disrupted in anxiety and depression.

Funding

This work was supported by the National Institutes of Health [grant number U01MH109985 under PAR-14-281].

Declaration of competing interest

The authors do not have any conflicts of interest to disclose.

Appendix A. Supplementary data

Supplementary data to this article can be found online at https://doi.org/10.1016/j.neuroimage.2020.116715.

References

Gorman, J.M., 1996. Comorbid depression and anxiety spectrum disorders. Depress. Anxiety 4, 160–168. https://doi.org/10.1002/(SICI)1520-6394(1996)4:4<160::AID-DA2>3.0.CO;2-J.

Ahmed, A.T., Frye, M.A., Rush, A.J., Biernacka, J.M., Craighead, W.E., McDonald, W.M., Bobo, W.V., Riva-Posse, P., Tye, S.J., Mayberg, H.S., Flavin, D.H., Skime, M.K., Jenkins, G.D., Wang, L., Krishnan, R.R., Weinshilboum, R.M., Kaddurah-Daouk, R., Dunlop, B.W., 2018. Mapping depression rating scale Phenotypes onto research domain criteria (RDoC) to inform biological research in mood disorders. J. Affect. Disord. 238, 1–7. https://doi.org/10.1016/j.jad.2018.05.005.

Balderston, N.L., Vytal, K.E., O'Connell, K., Torrisi, S., Letkiewicz, A., Ernst, M., Grillon, C., 2017. Anxiety patients show reduced working memory related dlPFC activation during safety and threat. Depress. Anxiety 34, 25–36. https://doi.org/10.1002/da.22518.

Barch, D.M., Burgess, G.C., Harms, M.P., Petersen, S.E., Schlaggar, B.L., Corbetta, M., Glasser, M.F., Curtiss, S., Dixit, S., Feldt, C., Nolan, D., Bryant, E., Hartley, T., Footer, O., Bjork, J.M., Poldrack, R., Smith, S., Johansen-Berg, H., Snyder, A.Z., Van Essen, D.C., 2013. Function in the human connectome: task-fMRI and individual differences in behavior. NeuroImage Mapp. Connectome 80, 169–189. https://doi.org/10.1016/j.neuroimage.2013.05.033.

Bartova, L., Meyer, B.M., Diers, K., Rabl, U., Scharinger, C., Popovic, A., Pail, G., Kalcher, K., Boubela, R.N., Huemer, J., Mandorfer, D., Windischberger, C., Sitte, H.H., Kasper, S., Praschak-Rieder, N., Moser, E., Brocke, B., Pezawas, L., 2015. Reduced default mode network suppression during a working memory task in remitted major depression. J. Psychiatr. Res. 64, 9–18. https://doi.org/10.1016/j.jpsychires.2015.02.025.

Beck, A.T., Epstein, N., Brown, G., Steer, R.A., 1988. An inventory for measuring clinical anxiety: psychometric properties. J. Consult. Clin. Psychol. 56, 893–897.

Beckmann, C.F., Smith, S.M., 2004. Probabilistic independent component analysis for functional magnetic resonance imaging. IEEE Trans. Med. Imag. 23, 137–152. https://doi.org/10.1109/TMI.2003.822821.

Berg, H.E., Ballard, E.D., Luckenbaugh, D.A., Nugent, A.C., Ionescu, D.F., Zarate, C.A., 2016. Recognition of emotional facial expressions in anxious and nonanxious depression. Compr. Psychiatr. 70, 1–8. https://doi.org/10.1016/j.comppsych.2016.06.007.

Burckhardt, C.S., Anderson, K.L., 2003. The quality of life scale (QOLS): reliability, validity, and utilization. Health Qual. Life Outcome 1, 60. https://doi.org/10.1186/1477-7525-1-60.

Bylsma, L.M., Morris, B.H., Rottenberg, J., 2008. A meta-analysis of emotional reactivity in major depressive disorder. Clin. Psychol. Rev. 28, 676–691. https://doi.org/10.1016/j.cpr.2007.10.001.

Carver, C.S., 1997. You want to measure coping but your protocol's too long: consider the brief COPE. Int. J. Behav. Med. 4, 92–100. https://doi.org/10.1207/s15327558ijbm0401_6.

Carver, C.S., White, T.L., 1994. Behavioral inhibition, behavioral activation, and affective responses to impending reward and punishment: the BIS/BAS scales. J. Pers. Soc. Psychol. 67, 319–333.
Cauley, S.F., Polimeni, J.R., Bhat, H., Wald, L.L., Setsompop, K., 2014. Interslice leakage artifact reduction technique for simultaneous multislice acquisitions. Magn. Reson. Med. 72, 93–102. https://doi.org/10.1002/mrm.24898.
Cole, M.W., Bassett, D.S., Power, J.D., Braver, T.S., Petersen, S.E., 2014. Intrinsic and task-evoked network architectures of the human brain. Neuron 83, 238–251. https://doi.org/10.1016/j.neuron.2014.05.014.
Cuthbert, B.N., Insel, T.R., 2013. Toward the future of psychiatric diagnosis: the seven pillars of RDoC. BMC Med. 11, 126. https://doi.org/10.1186/1741-7015-11-126.
Cuthbert, B.N., Kozak, M.J., 2013. Constructing constructs for psychopathology: the NIMH research domain criteria. J. Abnorm. Psychol. 122, 928–937. https://doi.org/10.1037/a0034028.
Dalili, M.N., Penton-Voak, I.S., Harmer, C.J., Munafò, M.R., 2015. Meta-analysis of emotion recognition deficits in major depressive disorder. Psychol. Med. 45, 1135–1144. https://doi.org/10.1017/S0033291714002591.
Diagnostic and statistical manual of mental disorders: DSM-5Tm, 5th ed, 2013. In: Diagnostic and Statistical Manual of Mental Disorders: DSM-5TM, fifth ed. American Psychiatric Publishing, Inc., Arlington, VA, US https://doi.org/10.1176/appi.books.9780890425596.
Dichter, G.S., Kozink, R.V., McClernon, F.J., Smoski, M.J., 2012. Remitted major depression is characterized by reward network hyperactivation during reward anticipation and hypoactivation during reward outcomes. J. Affect. Disord. 136, 1126–1134. https://doi.org/10.1016/j.jad.2011.09.048.
Elliott, R., Baker, S.C., Rogers, R.D., O'Leary, D.A., Paykel, E.S., Frith, C.D., Dolan, R.J., Sahakian, B.J., 1997a. Prefrontal dysfunction in depressed patients performing a complex planning task: a study using positron emission tomography. Psychol. Med. 27, 931–942.
Elliott, R., Sahakian, B., Herrod, J., Robbins, T., Paykel, E., 1997b. Abnormal response to negative feedback in unipolar depression: evidence for a diagnosis specific impairment. J. Neurol. Neurosurg. Psychiatry 63, 74–82.
Eshel, N., Roiser, J.P., 2010. Reward and punishment processing in depression. Biol. Psychiatr. 68, 118–124. https://doi.org/10.1016/j.biopsych.2010.01.027.
Fales, C.L., Barch, D.M., Burgess, G.C., Schaefer, A., Mennin, D.S., Gray, J.R., Braver, T.S., 2008. Anxiety and cognitive efficiency: differential modulation of transient and sustained neural activity during a working memory task. Cognit. Affect Behav. Neurosci. 8, 239–253.
Fonzo, G.A., Ramsawh, H.J., Flagan, T.M., Sullivan, S.G., Letamendi, A., Simmons, A.N., Paulus, M.P., Stein, M.B., 2015. Common and disorder-specific neural responses to emotional faces in generalised anxiety, social anxiety and panic disorders. Br. J. Psychiatry 206, 206–215. https://doi.org/10.1192/bjp.bp.114.149880.
Fortin, J.-P., Parker, D., Tunç, B., Watanabe, T., Elliott, M.A., Ruparel, K., Roalf, D.R., Satterthwaite, T.D., Gur, R.C., Gur, R.E., Schultz, R.T., Verma, R., Shinohara, R.T., 2017. Harmonization of multi-site diffusion tensor imaging data. Neuroimage 161, 149–170. https://doi.org/10.1016/j.neuroimage.2017.08.047.
Fox, M.D., Snyder, A.Z., Vincent, J.L., Corbetta, M., Essen, D.C.V., Raichle, M.E., 2005. The human brain is intrinsically organized into dynamic, anticorrelated functional networks. Proc. Natl. Acad. Sci. Unit. States Am. 102, 9673–9678. https://doi.org/10.1073/pnas.0504136102.
Fried, E.I., Nesse, R.M., 2015. Depression is not a consistent syndrome: an investigation of unique symptom patterns in the STAR*D study. J. Affect. Disord. 172, 96–102. https://doi.org/10.1016/j.jad.2014.10.010.
Glasser, M.F., Sotiropoulos, S.N., Wilson, J.A., Coalson, T.S., Fischl, B., Andersson, J.L., Xu, J., Jbabdi, S., Webster, M., Polimeni, J.R., Van Essen, D.C., Jenkinson, M., Wu-Minn Hcp Consortium, 2013. The minimal preprocessing pipelines for the Human Connectome Project. Neuroimage 80, 105–124. https://doi.org/10.1016/j.neuroimage.2013.04.127.
Goldstein-Piekarski, A.N., Williams, L.M., Humphreys, K., 2016. A trans-diagnostic review of anxiety disorder comorbidity and the impact of multiple exclusion criteria on studying clinical outcomes in anxiety disorders. Transl. Psychiatry 6, e847. https://doi.org/10.1038/tp.2016.108.
Greicius, M.D., Krasnow, B., Reiss, A.L., Menon, V., 2003. Functional connectivity in the resting brain: a network analysis of the default mode hypothesis. Proc. Natl. Acad. Sci. U.S.A. 100, 253–258. https://doi.org/10.1073/pnas.0135058100.
Grisanzio, K.A., Goldstein-Piekarski, A.N., Wang, M.Y., Rashed Ahmed, A.P., Samara, Z., Williams, L.M., 2018. Transdiagnostic symptom clusters and associations with brain, behavior, and daily function in mood, anxiety, and trauma disorders. JAMA Psychiatr. 75, 201–209. https://doi.org/10.1001/jamapsychiatry.2017.3951.
Haber, S.N., Knutson, B., 2010. The reward circuit: linking primate anatomy and human imaging. Neuropsychopharmacology 35, 4–26. https://doi.org/10.1038/npp.2009.129.
Hamilton, C.M., Strader, L.C., Pratt, J.G., Maiese, D., Hendershot, T., Kwok, R.K., Hammond, J.A., Huggins, W., Jackman, D., Pan, H., Nettles, D.S., Beaty, T.H., Farrer, L.A., Kraft, P., Marazita, M.L., Ordovas, J.M., Pato, C.N., Spitz, M.R., Wagener, D., Williams, M., Junkins, H.A., Harlan, W.R., Ramos, E.M., Haines, J., 2011a. The PhenX Toolkit: get the most from your measures. Am. J. Epidemiol. 174, 253–260. https://doi.org/10.1093/aje/kwr193.
Hamilton, J.P., Furman, D.J., Chang, C., Thomason, M.E., Dennis, E., Gotlib, I.H., 2011b. Default-mode and task-positive network activity in Major Depressive Disorder: implications for adaptive and maladaptive rumination. Biol. Psychiatr. 70, 327–333. https://doi.org/10.1016/j.biopsych.2011.02.003.
Hamilton, J.P., Etkin, A., Furman, D.J., Lemus, M.G., Johnson, R.F., Gotlib, I.H., 2012. Functional neuroimaging of major depressive disorder: a meta-analysis and new integration of baseline activation and neural response data. Aust. J. Pharm. 169, 693–703. https://doi.org/10.1176/appi.ajp.2012.11071105.
Hamilton, J.P., Farmer, M., Fogelman, P., Gotlib, I.H., 2015. Depressive rumination, the default-mode network, and the dark matter of clinical neuroscience. Biol. Psychiatr. 78, 224–230. https://doi.org/10.1016/j.biopsych.2015.02.020.
Hariri, A.R., Tessitore, A., Mattay, V.S., Fera, F., Weinberger, D.R., 2002. The amygdala response to emotional stimuli: a comparison of faces and scenes. Neuroimage 17, 317–323.
Harms, M.P., Somerville, L.H., Ances, B.M., Andersson, J., Barch, D.M., Bastiani, M., Bookheimer, S.Y., Brown, T.B., Buckner, R.L., Burgess, G.C., Coalson, T.S., Chappell, M.A., Dapretto, M., Douaud, G., Fischl, B., Glasser, M.F., Greve, D.N., Hodge, C., Jamison, K.W., Jbabdi, S., Kandala, S., Li, X., Mair, R.W., Mangia, S., Marcus, D., Mascali, D., Moeller, S., Nichols, T.E., Robinson, E.C., Salat, D.H., Smith, S.M., Sotiropoulos, S.N., Terpstra, M., Thomas, K.M., Tisdall, M.D., Ugurbil, K., van der Kouwe, A., Woods, R.P., Zöllei, L., Van Essen, D.C., Yacoub, E., 2018. Extending the human connectome project across ages: imaging protocols for the lifespan development and aging projects. Neuroimage 183, 972–984. https://doi.org/10.1016/j.neuroimage.2018.09.060.
Hasler, G., Drevets, W.C., Manji, H.K., Charney, D.S., 2004. Discovering endophenotypes for major depression. Neuropsychopharmacology 29, 1765–1781. https://doi.org/10.1038/sj.npp.1300506.
Hill, N.L., Mogle, J., Wion, R., Munoz, E., DePasquale, N., Yevchak, A.M., Parisi, J.M., 2016. Subjective cognitive impairment and affective symptoms: a systematic review. Gerontol. 56, e109–e127. https://doi.org/10.1093/geront/gnw091.
Hwang, J.W., Egorova, N., Yang, X.Q., Zhang, W.Y., Chen, J., Yang, X.Y., Hu, L.J., Sun, S., Tu, Y., Kong, J., 2015. Subthreshold depression is associated with impaired resting-state functional connectivity of the cognitive control network. Transl. Psychiatry 5, e683. https://doi.org/10.1038/tp.2015.174.
Hyvärinen, A., 1999. Fast and robust fixed-point algorithms for independent component analysis. IEEE Trans. Neural Network. 10, 626–634. https://doi.org/10.1109/72.761722.
Insel, T., Cuthbert, B., Garvey, M., Heinssen, R., Pine, D.S., Quinn, K., Sanislow, C., Wang, P., 2010. Research domain criteria (RDoC): toward a new classification framework for research on mental disorders. Am. J. Psychiatr. 167, 748–751. https://doi.org/10.1176/appi.ajp.2010.09091379.
Jaworska, N., Yang, X.-R., Knott, V., MacQueen, G., 2015. A review of fMRI studies during visual emotive processing in major depressive disorder. World J. Biol. Psychiatr. 16, 448–471. https://doi.org/10.3109/15622975.2014.885659.
Johnson, W.E., Li, C., Rabinovic, A., 2007. Adjusting batch effects in microarray expression data using empirical Bayes methods. Biostatistics 8, 118–127. https://doi.org/10.1093/biostatistics/kxj037.
Keren, H., O'Callaghan, G., Vidal-Ribas, P., Buzzell, G.A., Brotman, M.A., Leibenluft, E., Pan, P.M., Meffert, L., Kaiser, A., Wolke, S., Pine, D.S., Stringaris, A., 2018. Reward processing in depression: a conceptual and meta-analytic review across fMRI and EEG studies. Aust. J. Pharm. 175, 1111–1120. https://doi.org/10.1176/appi.ajp.2018.17101124.
Killgore, W.D.S., Britton, J.C., Schwab, Z.J., Price, L.M., Weiner, M.R., Gold, A.L., Rosso, I.M., Simon, N.M., Pollack, M.H., Rauch, S.L., 2014. Cortico-limbic responses to masked affective faces across ptsd, panic disorder, and specific phobia. Depress. Anxiety 31, 150–159. https://doi.org/10.1002/da.22156.
Knight, M.J., Baune, B.T., 2018. Cognitive dysfunction in major depressive disorder. Curr. Opin. Psychiatr. 31, 26–31. https://doi.org/10.1097/YCO.0000000000000378.
Kober, H., Barrett, L.F., Joseph, J., Bliss-Moreau, E., Lindquist, K., Wager, T.D., 2008. Functional grouping and cortical-subcortical interactions in emotion: a meta-analysis of neuroimaging studies. Neuroimage 42, 998–1031. https://doi.org/10.1016/j.neuroimage.2008.03.059.
Korgaonkar, M.S., Grieve, S.M., Etkin, A., Koslow, S.H., Williams, L.M., 2013. Using standardized fMRI protocols to identify patterns of prefrontal circuit dysregulation that are common and specific to cognitive and emotional tasks in major depressive disorder: first wave results from the iSPOT-D study. Neuropsychopharmacology 38, 863–871. https://doi.org/10.1038/npp.2012.252.
Kunisato, Y., Okamoto, Y., Ueda, K., Onoda, K., Okada, G., Yoshimura, S., Suzuki, S., Samejima, K., Yamawaki, S., 2012. Effects of depression on reward-based decision making and variability of action in probabilistic learning. J. Behav. Ther. Exp. Psychiatr. 43, 1088–1094. https://doi.org/10.1016/j.jbtep.2012.05.007.
Lam, R.W., Kennedy, S.H., McIntyre, R.S., Khullar, A., 2014. Cognitive dysfunction in major depressive disorder: effects on psychosocial functioning and implications for treatment. Can. J. Psychiatr. 59, 649–654.
Lee, R.S.C., Hermens, D.F., Porter, M.A., Redoblado-Hodge, M.A., 2012. A meta-analysis of cognitive deficits in first-episode Major Depressive Disorder. J. Affect. Disord. 140, 113–124. https://doi.org/10.1016/j.jad.2011.10.023.
Lerma-Usabiaga, G., Mukherjee, P., Ren, Z., Perry, M.L., Wandell, B.A., 2019a. Replication and generalization in applied neuroimaging. Neuroimage 202, 116048. https://doi.org/10.1016/j.neuroimage.2019.116048.
Lerma-Usabiaga, G., Perry, M.L., Wandell, B.A., 2019b. Reproducible Tract Profiles (RTP): from diffusion MRI acquisition to publication. bioRxiv. https://doi.org/10.1101/680173, 680173.
Milders, M., Bell, S., Platt, J., Serrano, R., Runcie, O., 2010. Stable expression recognition abnormalities in unipolar depression. Psychiatr. Res. 179, 38–42. https://doi.org/10.1016/j.psychres.2009.05.015.
Morosini, P.L., Magliano, L., Brambilla, L., Ugolini, S., Pioli, R., 2000. Development, reliability and acceptability of a new version of the DSM-IV Social and Occupational Functioning Assessment Scale (SOFAS) to assess routine social functioning. Acta Psychiatr. Scand. 101, 323–329. https://doi.org/10.1034/j.1600-0447.2000.101004323.x.
Murphy, S.L., Xu, J., Kochanek, K.D., Curtin, S.C., Arias, E., 2017. Deaths: final data for 2015. Natl. Vital Stat. Rep. 66, 1–75.

Niendam, T.A., Laird, A.R., Ray, K.L., Dean, Y.M., Glahn, D.C., Carter, C.S., 2012. Meta-analytic evidence for a superordinate cognitive control network subserving diverse executive functions. Cognit. Affect Behav. Neurosci. 12, 241–268. https://doi.org/10.3758/s13415-011-0083-5.

Parola, N., Zendjidjian, X.Y., Alessandrini, M., Baumstarck, K., Loundou, A., Fond, G., Berna, F., Lançon, C., Auquier, P., Boyer, L., 2017. Psychometric properties of the Ruminative Response Scale-short form in a clinical sample of patients with major depressive disorder. Patient Prefer. Adherence 11, 929–937. https://doi.org/10.2147/PPA.S125730.

Pechtel, P., Dutra, S.J., Goetz, E.L., Pizzagalli, D.A., 2013. Blunted reward responsiveness in remitted depression. J. Psychiatr. Res. 47, 1864–1869. https://doi.org/10.1016/j.jpsychires.2013.08.011.

Pestilli, F., Yeatman, J.D., Rokem, A., Kay, K.N., Wandell, B.A., 2014. Evaluation and statistical inference for living connectomes. Nat. Methods 11, 1058–1063. https://doi.org/10.1038/nmeth.3098.

Phillips, M.L., Drevets, W.C., Rauch, S.L., Lane, R., 2003. Neurobiology of emotion perception II: implications for major psychiatric disorders. Biol. Psychiatr. 54, 515–528. https://doi.org/10.1016/S0006-3223(03)00171-9.

Price, J.L., Drevets, W.C., 2009. Neurocircuitry of mood disorders. Neuropsychopharmacology 35, 192–216. https://doi.org/10.1038/npp.2009.104.

Qiu, C., Liao, W., Ding, J., Feng, Y., Zhu, C., Nie, X., Zhang, W., Chen, H., Gong, Q., 2011. Regional homogeneity changes in social anxiety disorder: a resting-state fMRI study. Psychiatr. Res. 194, 47–53. https://doi.org/10.1016/j.pscychresns.2011.01.010.

Raichle, M.E., 2015. The brain's default mode network. Annu. Rev. Neurosci. 38, 433–447. https://doi.org/10.1146/annurev-neuro-071013-014030.

Robinson, O.J., Krimsky, M., Lieberman, L., Allen, P., Vytal, K., Grillon, C., 2014. The dorsal medial prefrontal (anterior cingulate) cortex–amygdala aversive amplification circuit in unmedicated generalised and social anxiety disorders: an observational study. Lancet Psychiatr. 1, 294–302. https://doi.org/10.1016/S2215-0366(14)70305-0.

Rock, P.L., Roiser, J.P., Riedel, W.J., Blackwell, A.D., 2014. Cognitive impairment in depression: a systematic review and meta-analysis. Psychol. Med. 44, 2029–2040. https://doi.org/10.1017/S0033291713002535.

Roehrig, C., 2016. Mental disorders top the list of the most costly conditions in the United States: $201 billion. Health Aff. 35, 1130–1135. https://doi.org/10.1377/hlthaff.2015.1659.

Sanchez, A., Romero, N., Maurage, P., De Raedt, R., 2017. Identification of emotions in mixed disgusted-happy faces as a function of depressive symptom severity. J. Behav. Ther. Exp. Psychiatr. 57, 96–102. https://doi.org/10.1016/j.jbtep.2017.05.002.

Setsompop, K., Gagoski, B.A., Polimeni, J.R., Witzel, T., Wedeen, V.J., Wald, L.L., 2012. Blipped-controlled aliasing in parallel imaging for simultaneous multislice echo planar imaging with reduced g-factor penalty. Magn. Reson. Med. 67, 1210–1224. https://doi.org/10.1002/mrm.23097.

Sheehan, D.V., Lecrubier, Y., Sheehan, K.H., Amorim, P., Janavs, J., Weiller, E., Hergueta, T., Baker, R., Dunbar, G.C., 1998. The Mini-International Neuropsychiatric Interview (M.I.N.I.): the development and validation of a structured diagnostic psychiatric interview for DSM-IV and ICD-10. J. Clin. Psychiatr. 59 (Suppl. 20), 22–33 quiz 34-57.

Sheline, Y.I., Price, J.L., Yan, Z., Mintun, M.A., 2010. Resting-state functional MRI in depression unmasks increased connectivity between networks via the dorsal nexus. Proc. Natl. Acad. Sci. U.S.A. 107, 11020–11025. https://doi.org/10.1073/pnas.1000446107.

Shen, T., Li, C., Wang, B., Yang, W., Zhang, C., Wu, Z., Qiu, M., Liu, J., Xu, Y., Peng, D., 2015. Increased cognition connectivity network in major depression disorder: a fMRI study. Psychiatr. Invest. 12, 227–234. https://doi.org/10.4306/pi.2015.12.2.227.

Siegle, G.J., Thompson, W., Carter, C.S., Steinhauer, S.R., Thase, M.E., 2007. Increased amygdala and decreased dorsolateral prefrontal BOLD responses in unipolar depression: related and independent features. Biol. Psychiatr. 61, 198–209. https://doi.org/10.1016/j.biopsych.2006.05.048.

Silverstein, S.M., Berten, S., Olson, P., Paul, R., Williams, L.M., Cooper, N., Gordon, E., 2007. Development and validation of a World-Wide-Web-based neurocognitive assessment battery: WebNeuro. Behav. Res. Methods 39, 940–949. https://doi.org/10.3758/BF03192989.

Somerville, L.H., Bookheimer, S.Y., Buckner, R.L., Burgess, G.C., Curtiss, S.W., Dapretto, M., Elam, J.S., Gaffrey, M.S., Harms, M.P., Hodge, C., Kandala, S., Kastman, E.K., Nichols, T.E., Schlaggar, B.L., Smith, S.M., Thomas, K.M., Yacoub, E., Van Essen, D.C., Barch, D.M., 2018. The Lifespan Human Connectome Project in Development: a large-scale study of brain connectivity development in 5-21 year olds. Neuroimage 183, 456–468. https://doi.org/10.1016/j.neuroimage.2018.08.050.

Spreng, R.N., Sepulcre, J., Turner, G.R., Stevens, W.D., Schacter, D.L., 2013. Intrinsic architecture underlying the relations among the default, dorsal attention, and frontoparietal control networks of the human brain. J. Cognit. Neurosci. 25, 74–86. https://doi.org/10.1162/jocn_a_00281.

Takemura, H., Caiafa, C.F., Wandell, B.A., Pestilli, F., 2016. Ensemble tractography. PLoS Comput. Biol. 12, e1004692 https://doi.org/10.1371/journal.pcbi.1004692.

Tournier, J.-D., Smith, R., Raffelt, D., Tabbara, R., Dhollander, T., Pietsch, M., Christiaens, D., Jeurissen, B., Yeh, C.-H., Connelly, A., 2019. MRtrix3: a fast, flexible and open software framework for medical image processing and visualisation. Neuroimage 202, 116137. https://doi.org/10.1016/j.neuroimage.2019.116137.

Treadway, M.T., Zald, D.H., 2011. Reconsidering anhedonia in depression: lessons from translational neuroscience. Neurosci. Biobehav. Rev. 35, 537–555. https://doi.org/10.1016/j.neubiorev.2010.06.006.

Van Essen, D.C., Barch, D.M., 2015. The human connectome in health and psychopathology. World Psychiatr. 14, 154–157. https://doi.org/10.1002/wps.20228.

Van Essen, D.C., Smith, S.M., Barch, D.M., Behrens, T.E.J., Yacoub, E., Ugurbil, K., Wu-Minn Hcp Consortium, 2013. The Wu-Minn human connectome project: an overview. Neuroimage 80, 62–79. https://doi.org/10.1016/j.neuroimage.2013.05.041.

Vasic, N., Walter, H., Sambataro, F., Wolf, R.C., 2009. Aberrant functional connectivity of dorsolateral prefrontal and cingulate networks in patients with major depression during working memory processing. Psychol. Med. 39, 977–987. https://doi.org/10.1017/S0033291708004443.

Vrieze, E., Pizzagalli, D.A., Demyttenaere, K., Hompes, T., Sienaert, P., de Boer, P., Schmidt, M., Claes, S., 2013. Reduced reward learning predicts outcome in major depressive disorder. Biol. Psychiatr. 73, 639–645. https://doi.org/10.1016/j.biopsych.2012.10.014.

Walters, M., Hines-Martin, V., 2018. Overview of executive functions in mood and depressive disorders: a review of the literature. Arch. Psychiatr. Nurs. 32, 617–637. https://doi.org/10.1016/j.apnu.2018.02.011.

Wardenaar, K.J., van Veen, T., Giltay, E.J., de Beurs, E., Penninx, B.W.J.H., Zitman, F.G., 2010. Development and validation of a 30-item short adaptation of the mood and anxiety symptoms questionnaire (MASQ). Psychiatr. Res. 179, 101–106. https://doi.org/10.1016/j.psychres.2009.03.005.

Watson, D., Clark, L.A., Tellegen, A., 1988. Development and validation of brief measures of positive and negative affect: the PANAS scales. J. Pers. Soc. Psychol. 54, 1063–1070.

Watters, A.J., Williams, L.M., 2011. Negative biases and risk for depression; integrating self-report and emotion task markers. Depress. Anxiety 28, 703–718. https://doi.org/10.1002/da.20854.

Weintraub, S., Dikmen, S.S., Heaton, R.K., Tulsky, D.S., Zelazo, P.D., Bauer, P.J., Carlozzi, N.E., Slotkin, J., Blitz, D., Wallner-Allen, K., Fox, N.A., Beaumont, J.L., Mungas, D., Nowinski, C.J., Richler, J., Deocampo, J.A., Anderson, J.E., Manly, J.J., Borosh, B., Havlik, R., Conway, K., Edwards, E., Freund, L., King, J.W., Moy, C., Witt, E., Gershon, R.C., 2013. Cognition assessment using the NIH Toolbox. Neurology 80, S54–S64. https://doi.org/10.1212/WNL.0b013e3182872ded.

Wessa, M., Lois, G., 2015. Brain functional effects of psychopharmacological treatment in major depression: a focus on neural circuitry of affective processing. Curr. Neuropharmacol. 13, 466–479. https://doi.org/10.2174/1570159X13666150416224801.

Whiteford, H.A., Degenhardt, L., Rehm, J., Baxter, A.J., Ferrari, A.J., Erskine, H.E., Charlson, F.J., Norman, R.E., Flaxman, A.D., Johns, N., Burstein, R., Murray, C.J.L., Vos, T., 2013. Global burden of disease attributable to mental and substance use disorders: findings from the Global Burden of Disease Study 2010. Lancet 382, 1575–1586. https://doi.org/10.1016/S0140-6736(13)61611-6.

Williams, L.M., 2016. Precision psychiatry: a neural circuit taxonomy for depression and anxiety. Lancet Psychiatr. 3, 472–480. https://doi.org/10.1016/S2215-0366(15)00579-9.

Williams, L.M., 2017. Defining biotypes for depression and anxiety based on large-scale circuit dysfunction: a theoretical review of the evidence and future directions for clinical translation. Depress. Anxiety 34, 9–24. https://doi.org/10.1002/da.22556.

Williams, L.M., Goldstein-Piekarski, A.N., Chowdhry, N., Grisanzio, K.A., Haug, N.A., Samara, Z., Etkin, A., O'Hara, R., Schatzberg, A.F., Suppes, T., Yesavage, J., 2016. Developing a clinical translational neuroscience taxonomy for anxiety and mood disorder: protocol for the baseline-follow up Research domain criteria Anxiety and Depression ("RAD") project. BMC Psychiatr. 16 https://doi.org/10.1186/s12888-016-0771-3.

Winkler, A.M., Ridgway, G.R., Webster, M.A., Smith, S.M., Nichols, T.E., 2014. Permutation inference for the general linear model. Neuroimage 92, 381–397. https://doi.org/10.1016/j.neuroimage.2014.01.060.

Woolrich, M.W., Ripley, B.D., Brady, M., Smith, S.M., 2001. Temporal autocorrelation in univariate linear modeling of FMRI data. Neuroimage 14, 1370–1386. https://doi.org/10.1006/nimg.2001.0931.

Yarkoni, T., Poldrack, R.A., Nichols, T.E., Van Essen, D.C., Wager, T.D., 2011. Large-scale automated synthesis of human functional neuroimaging data. Nat. Methods 8, 665–670. https://doi.org/10.1038/nmeth.1635.

Yeatman, J.D., Dougherty, R.F., Myall, N.J., Wandell, B.A., Feldman, H.M., 2012. Tract profiles of white matter properties: automating fiber-tract quantification. PloS One 7. https://doi.org/10.1371/journal.pone.0049790.

Zhang, W.-N., Chang, S.-H., Guo, L.-Y., Zhang, K.-L., Wang, J., 2013. The neural correlates of reward-related processing in major depressive disorder: a meta-analysis of functional magnetic resonance imaging studies. J. Affect. Disord. 151, 531–539. https://doi.org/10.1016/j.jad.2013.06.039.